Accepted Manuscript

Development of a novel series of non-natural triaryl agonists and antagoinsts of the *Pseudomonas aeruginosa* LasR quorum sensing receptor

Joseph N. Capilato, Shane Philippi, Thomas Reardon, Ashleigh McConnell, Dylan Oliver, Amy Warren, Jill Adams, Chun Wu, Lark J. Perez

PII: S0968-0896(16)30741-6
DOI: http://dx.doi.org/10.1016/j.bmc.2016.10.021
Reference: BMC 13348

To appear in: *Bioorganic & Medicinal Chemistry*

Received Date: 16 September 2016
Revised Date: 13 October 2016
Accepted Date: 17 October 2016

Please cite this article as: Capilato, J.N., Philippi, S., Reardon, T., McConnell, A., Oliver, D., Warren, A., Adams, J., Wu, C., Perez, L.J., Development of a novel series of non-natural triaryl agonists and antagoinsts of the *Pseudomonas aeruginosa* LasR quorum sensing receptor, *Bioorganic & Medicinal Chemistry* (2016), doi: http://dx.doi.org/10.1016/j.bmc.2016.10.021

Graphical Abstract

To create your abstract, type over the instructions in the template box below.
Fonts or abstract dimensions should not be changed or altered.

Development of a Novel Series of Non-natural Triaryl Agonists and Antagoinsts of the *Pseudomonas aeruginosa* LasR Quorum Sensing Receptor

Leave this area blank for abstract info.

Joseph N. Capilato, Shane Philippi, Thomas Reardon, Ashleigh McConnell, Dylan Oliver, Amy Warren, Jill Adams, Chun Wu and Lark J. Perez*

Department of Chemistry and Biochemistry, Rowan University, 201 Mullica Hill Road, Glassboro, NJ 08028, United States

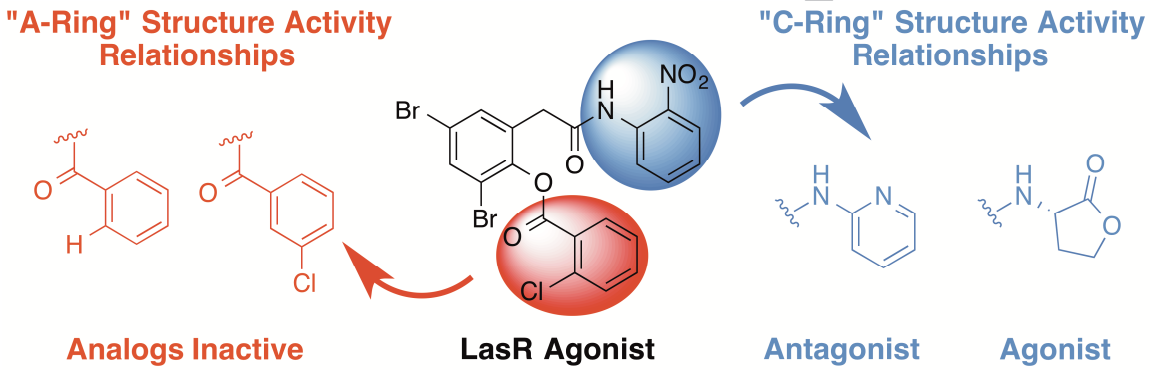

Bioorganic & Medicinal Chemistry
journal homepage: www.elsevier.com

Development of a novel series of non-natural triaryl agonists and antagoinsts of the *Pseudomonas aeruginosa* LasR quorum sensing receptor

Joseph N. Capilato, Shane Philippi, Thomas Reardon, Ashleigh McConnell, Dylan Oliver, Amy Warren, Jill Adams, Chun Wu and Lark J. Perez*

[a] *Department of Chemistry and Biochemistry, Rowan University, 201 Mullica Hill Road, Glassboro, NJ 08028, United States*

ARTICLE INFO

Article history:
Received
Received in revised form
Accepted
Available online

Keywords:
Anti-virulence
Pseudomonas aeruginosa
Structure-activity relationship
Computational Modeling
Quorum sensing

ABSTRACT

Bacterial chemical communication, through a process called quorum sensing (QS), plays a central role in infection in numerous bacterial pathogens. Quorum sensing in Pseudomonas aeruginosa employs a series of small molecule receptors including the master QS regulator, LasR. In this study we investigate a non-natural triaryl series of LasR ligands using a combination of structure activity relationship studies and computational modeling. These studies have enabled the identification of key structural requirements for ligand binding and have revealed a new strategy for inducing the therapeutically relevant antagonism of LasR.

1. Introduction

Due to the array of medically relevant cellular processes that are under the control of LuxR-type quorum sensing circuits, significant effort has been directed toward the identification of antagonist and agonist molecules in several different bacterial pathogens.[1-3] These efforts have led to the identification of antagonists and agonists of quorum sensing from natural sources,[4] diversity-oriented compound libraries,[5,6] and focused library synthesis.[7,8] The most broadly explored class of LuxR-type receptor ligands are based on the structural features found in the native HSLs (e.g. **1**, Figure 1). The wealth of studies in this area, maintaining the homoserine lactone while changing the functionality of the acyl-tail is facilitated by ready synthesis of the HSL compound libraries. Together these investigations targeting the modulation of quorum sensing in Gram-negative bacteria have yielded numerous promising results and insightful structure activity relationships.[9,10]

The inhibition of quorum sensing with small molecules offers a unique strategy for the treatment and prevention of a number of acute and chronic bacterial infections, a fact that is of particular significance given the rapid and ongoing spread of antimicrobial-resistant bacteria.[2,11,12] Through the inhibition of quorum sensing, control over expression of virulence factors and biofilm formation is achieved, rendering the bacteria benign while not directly affecting viability. This anti-infective approach is conceptually distinct from traditional approaches for the treatment of bacterial infection that typically utilize bactericidal or bacteriostatic molecules, targeting critical cellular processes. As exemplified by the spread of bacterial resistance, these treatments provide a considerable growth advantage to bacteria that can resist the drug. Contrasting this approach, the inhibition of quorum sensing does not affect cellular viability, decreasing the growth advantage of resistance.[13] Rather, this approach targets cellular signaling, inhibiting the expression of virulence factors necessary for successful infection, rendering the bacteria benign until the hosts immune system can clear the pathogen.[2,14-16]

Major challenges that remain in the development of an anti-quorum sensing strategy targeting the development of antagonists of LasR and other LuxR-type receptors is ligand potency and the complications of hydrolytic liability in HSL-based antagonists.[17] Here we advance a strategy to overcome the limitation of inhibitor potency through the exploration of a novel, non-natural triaryl series of LasR quorum sensing ligands. Further, many of the analogs examined in this study are anticipated to overcome the limitations of the HSL-based agonists and antagonists by removing the physiologically labile homoserine lactone functionality.[18]

Recently a highly potent agonist of quorum-sensing in *P. aeruginosa* was identified from a high-throughput screen (**2**, Figure 2).[5] While the activation of virulence factor expression in this bacterial pathogen is not therapeutically desirable our rationale to obtain the desired inhibitory function for this potent agonist through analog synthesis is based on precedent. Most notably, a large number of inhibitors have been discovered by systematic modification of HSLs, molecules which serve as natural QS activators. The agonist discovered (**2**) bears many structural and pharmacological properties that potentially make it

superior to HSLs as a lead compound for the development of an anti-virulence therapy, including the absence of the metabolically labile homoserine lactone. Additionally, the potency of this molecule for activation of LasR is comparable to the potency of the natural signaling molecule; however, compounds of this structure type have never been systematically analyzed for the effect of their structure-activity relationships (SARs).[5,19] Here we describe the first systematic evaluation of the structure-activity relationships of this novel class of LasR QS modulators. Our studies reveal critical details of the activity profile of this new ligand class for LasR activity and using computational modeling we provide insight into the molecular interactions with LasR that contribute to agonist and antagonist activity.

2. Library Synthesis.

Challenging our efforts toward the goal of identifying inhibitors of LasR based on the structure of **2** is the number of synthetic steps required for its assembly (Figure 1).[19] Previous studies had described an eight step synthesis of **2**, however, to prepare a library of molecules related to **2** ideally required a more efficient synthetic route. Identification of an alternative scaffold to target for structure-activity relationship studies was informed by examination of the recently published crystal structure of the QS receptor in *P. aeruginosa*, LasR, in the presence of **2**.[20] Analysis of the binding pocket for the ligand suggested that a subtle structural change in the orientation of the amide bond in **2** (Figure 1, highlighted in blue) may be tolerated. Indeed, examination of the scaffold resulting from the inversion of the amide linker between the "B-ring" and "C-ring" (highlighted in red, **3**) more closely maps onto the orientation of this structure in the native LasR agonist, 3-oxo-C12HSL (**1**).

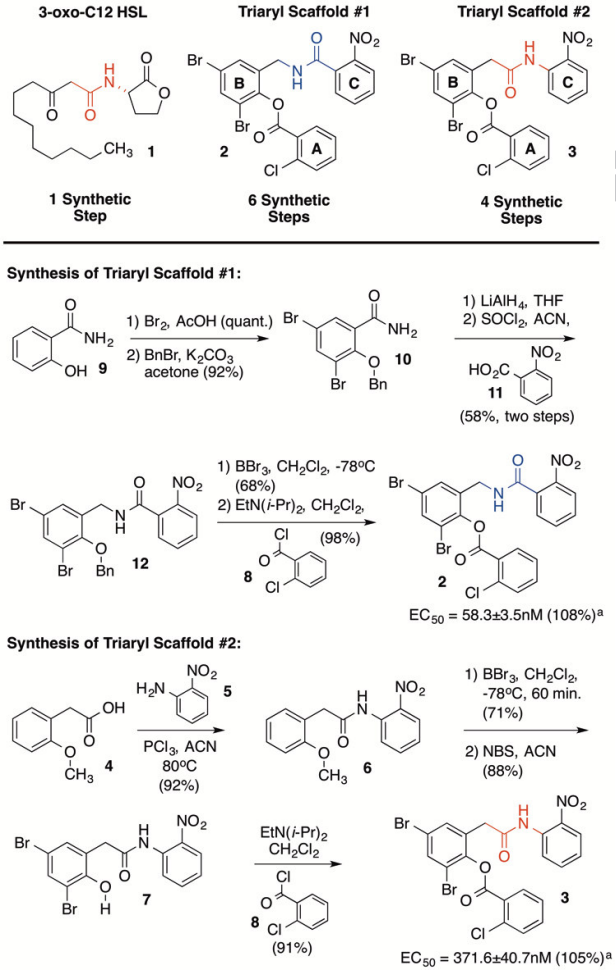

Figure 1. Top; the structures of the native agonist of the QS receptor, LasR, 3-oxo-C12HSL and the triaryl scaffolds evaluated as LasR agonists and antagonists in this study. Bottom; a description of the modular chemical synthesis pathways for library assembly.

Based on these target scaffolds, we have successfully identified two efficient and modular synthetic routes (Figure 1) to analogs containing the core scaffold as in **2** (Scaffold #1) analogs containing the core scaffold as in **3** (Scaffold #2). In our optimized six step synthesis of **2** and analogs of this structure, bromination and benzyl protection of salicylamide is followed by reduction of the amide and introduction of the "C-ring" through amidation with **11**. Final incorporation of the "A-ring" is achieved through deprotection of the phenol and esterification with **8**. This route is modular, enabling ready diversification of the "A-ring" and "C-ring" of the ligand and proceeds in 35% yield overall from salicylamide. The synthesis of **3** and related analogs involves initial coupling of **4** and 2-nitro aniline (**5**). Deprotection of the phenol and bromination of the more electron rich "B-ring" proceeds smoothly to provide **7** which can be directly esterified with **8**. Overall, this route allows rapid diversification of the "A-ring" and "C-ring" of **3**, proceeding in four steps with 52% overall yield from **4**.

3. Library Design and SAR.

Analysis of the crystal structure of LasR complexed to **2**[20] suggests that the two terminal aromatic rings (Figure 1, labeled "**A**" and "**C**") play an important role by interacting with LasR whereas the central ring appears to play primarily a scaffolding role in ligand binding. Therefore, we have focused our initial efforts on identifying the structure activity correlations of the pendant ring structures ("A-ring" and "C-ring") while maintaining the structure of the central ring ("B-ring"). Our strategy involved initial broad investigation of structure-activity relationships in the more readily synthesized ligand series (Scaffold #2, e.g. **3**) before returning to investigate key analogs prepared based on Scaffold #1. While the two scaffolds differ only in the orientation of one amide bond, we have observed some notable differences in biological activity for analogs prepared on the two different scaffolds.

3.1. "A-ring" SAR and computational analysis.

Our initial investigations of the structure activity relationships involved modulation of the structure of the "A-ring" in Scaffold #2. From this series of structural analogs, we observe a consistent dependence of substitution in this ring structure on the potency of the molecules (Table 1). We discovered that substitution in the *ortho*-position of the arene (entries 1, 4, 7, 9, 10, and 13-14) is critical for agonist activity. Interestingly, the activity of the analogs bearing *ortho*-substitution appears to be largely independent of the nature of the substituent. Analogs with electon-withdrawing substituents (halogen, nitro, trifluoromethyl) and electron-donating groups (methyl, methoxy) in the *ortho*-position all are agonists with EC_{50} values between 2.4 and 15.8 μM. By contrast to substitution in the *ortho*-position of the "A-ring", substitution in the *meta*- or *para*-position of the "A-ring" (entries 2-3, 5-7 and 11-12) leads to the complete loss of activity. In support of the significance of *ortho*-substitution, an analog was prepared containing chlorine atoms at both of the *ortho*-positions of the "A-ring" (entry 16) fully retains the activity of the mono-*ortho*-chloro LasR agonist **3**. We additionally find that the carbonyl of the ester is not significant for agonist activity as an analog removing this functionality, linking the "A-ring" through an ether linker (**28,** entry 17) retains full agonist activity.

Table 1. Structure-activity relationships of "A-ring" analogs.

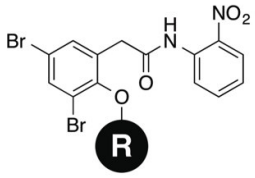

Entry	Structure	EC_{50} (μM)[a]	% Max[b]	Entry	Structure	EC_{50} (μM)[a]	% Max[b]
1	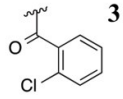 **3**	0.372±0.041	105	10	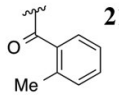 **21**	0.757±0.065	85
2	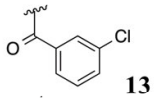 **13**	>50.0	0	11	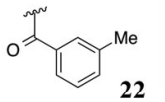 **22**	>50.0	24
3	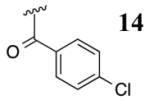 **14**	>50.0	0	12	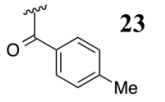 **23**	>50.0	33
4	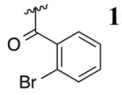 **15**	0.271±0.022	82	13	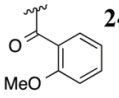 **24**	0.246±0.012	45
5	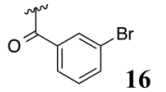 **16**	>50.0	44	14	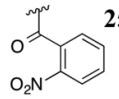 **25**	0.489±1.28	37
6	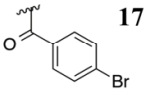 **17**	>50.0	35	15	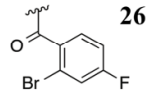 **26**	0.436±0.550	100
7	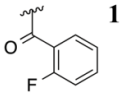 **18**	1.29±0.598	76	16	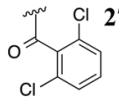 **27**	0.313±0.149	95
8	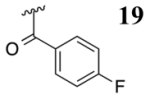 **19**	>50.0	39	17	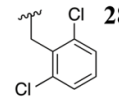 **28**	0.161±0.101	56
9	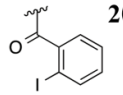 **20**	1.58±0.046	50	18	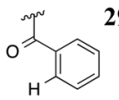 **29**	>50.0	0

[a] EC_{50} values are reported as the mean of triplicate analysis with the range defining the standard deviation. The native LasR agonist (**1**) was used as a control with an EC_{50}=72.9±24.6nM. [b] Maximal percent activation of GFP at 50 μM with respect to 3-oxo-C12 HSL (**1**) as a positive control for LasR agonism, set at 100% activation.

Generally we find that analogs with substituents in the *ortho*-position are potent agonists whereas the *meta*- or *para*-substituted analogs are universally not active. This may suggest that the binding pocket in LasR for this portion of the molecule is not able to accommodate substituents in either the *meta*- or *para*-position. Further, the comparable activities of the analogs containing electronically and sterically diverse substituents in the *ortho*-position suggests that this substitution does not have a direct role interacting with the receptor (no specific hydrogen-bonding or electronic interactions with the receptor) but rather

may simply play an anchoring role for the overall positioning of the "A-ring". In support of this hypothesis, analog **26**, containing an *ortho*-bromo substituent and a *para*-fluoro substituent is active as a LasR agonist (entry 15), while the analog containing the para-fluoro substituent alone is inactive (entry 8). Further supporting the significance of maintaining an *ortho*-substituent on the "A-ring" is the lack of agonist activity found in analog **29** (entry 18) that possesses an unsubstituted phenyl ring at this position.

The ligands that were inactive as agonists in this series were further evaluated as antagonists and were found to have no antagonist activity. This observation suggests that the presence of minimally one *ortho* substituent on the "A-ring" of ligands in this series is required for ligand binding to LasR in the cell.

To further investigate the strict requirement for the presence of an *ortho*-substituent on the "A-ring" for LasR agonist activity we performed computational binding studies using the Schrodinger Drug Discovery Suite. We were pleased to find that the MMGBSA scores (measure of binding affinity) from this computational binding analysis for the full series of compounds in Table 1 was strongly correlated to the observed biological activity of the analogs with the *ortho*-substituted analogs showing the strongest binding and the unsubstituted phenyl "A-ring" analog (**29**) predicted to be a poor LasR ligand (Table 2).

Table 2. Calculated binding energies for "A-ring" analogs.

	MMGBSA Binding Energy (kcal/mol)
Ortho-Substituted Analogs[a]	–87.12±20.87[d]
Meta-Substituted Analogs[b]	–37.35±6.15[d]
Para-Substituted Analogs[c]	–18.86±27.79[d]
Unsubstituted Phenyl Analog **29**	–11.05

[a] Average calculated binding energy of analogs **3**, **15**, **18**, **20**, **21**, **24** and **25**. [b] Average calculated binding energy of analogs **13**, **16** and **22**. [c] Average calculated binding energy of analogs **14**, **17**, **19** and **23**. [d] MMGBSA is reported as the average binding energy with the error representing standard deviation.

Building on this result we computationally investigated the relative contributions for each of the amino acids within the LasR binding pocket that, in sum, contribute to the overall MMGBSA score for the compound. We hypothesized that this analysis may enable the identification of key residues in LasR that contribute to ligand binding rationalizing that the *meta*- and *para*-substituted "A-ring" analogs would lack these stabilizing interactions or would display destabilizing interactions. We identified several individual amino acids that showed variations in their extracted contribution to the computational binding energies (Figure 2).

Generally, amino acids residues proximal to the 2-nitro aniline "C-ring" of the analog, not varied in this series of analogs, displayed similar binding energies to each of the ligands, irrespective of the substitution pattern on the "A-ring". For example, W60 and F101 (Figure 3, light blue) independently contribute stabilizing binding interactions to all of the analogs evaluated (Figure 2).

Some variations in the extracted binding energies are noted in the amino acid residues responsible for interactions with the amide linker between the "C-ring" and "B-ring" of the analogs. Amino acid residues which are highly conserved among soluble

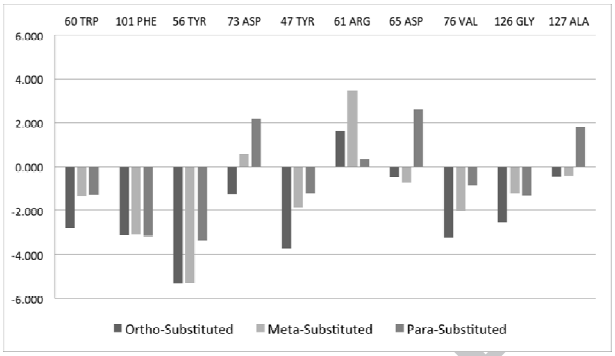

Figure 2. Computational binding contributions of individual amino acids in LasR with the ligands in Table 1. Energies are described in kcal/mol.

HSL-binding proteins, Y56 and D73 (Figure 3, yellow), display different patterns of binding between the analogs dependent on the substitution of the "A-ring". While Y56 shows strongly stabilizing interactions with all analogs, by virtue of a hydrogen bond to the carbonyl oxygen of the linker amide, this stabilizing interaction appears to be slightly weakened in the binding of the *para*-substituted ligands (Figure 2). In contrast, the interactions between the ligand and D73 are calculated to be generally low in energy with *ortho*- and *meta*-substituted analogs however becomes significantly destabilizing in interactions with ligands bearing a *para*-substituent in the "A-ring". Apparently, substitution in the *para*-position of the distant "A-ring" is effectively propagated through the ligand to disrupt the hydrogen bonding interactions between LasR and the linker amide of the ligand.

Not surprisingly, a series of amino acids in the binding pocket proximal to the "A-ring" were found to be most significantly influenced by the structural changes investigated in this ligand series. While much of this large portion of the HSL binding pocket in LasR is hydrophobic, key amino acids displaying significant differences in binding to the structural variations in the "A-ring" include Y47, R61, D65, V76, G126 and A127 (Figure 3, magenta). Two primary trends are noted in the binding contribution of amino acids in this region of LasR. Firstly, in stabilizing interactions the *ortho*-substituted analogs show greater stabilization then *meta*- or *para*-substituted analogs. This trend is

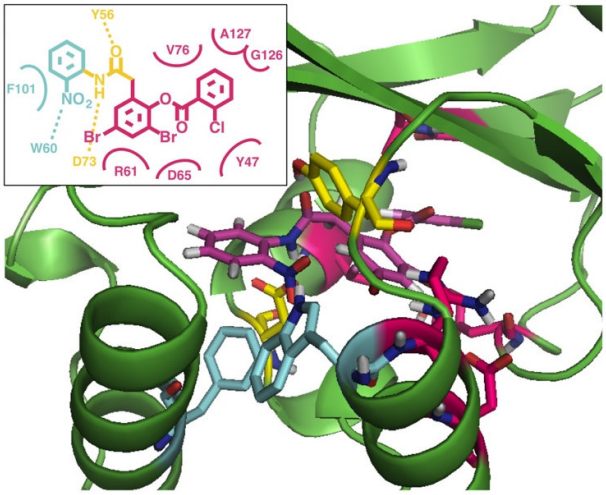

Figure 3. Key residues in LasR shown with 3 docked. W60 and F101 are shown in light blue, Y56 and D73 are shown in yellow and Y47, R61, D65, V76, G126 and A127 are shown in magenta. Inset: a schematic representation highlighting these amino acids in proximity to three regions of the ligand.

exemplified in the binding contributions of Y47, V76 and G126 (Figure 2). Secondly, two residues show strong destabilizing interactions uniquely with the *para*-substituted analogs, D65 and A127 (Figure 3). These residues are located on opposing sides of the binding pocket possibly suggesting that a steric clash on one side of the ligand binding pocket pushes the ligand toward the opposing side of the binding pocket resulting in destabilizing interactions with these two spatially separated amino acids. Lastly, it should be noted that not all amino acids showed a preference for the *ortho*-substituted analogs. One residue analyzed, R61 shows significant destabilizing interactions with both *ortho*- and *meta*-substituted analogs that is alleviated in the *para*-substituted series of compounds.

3.2. "C-ring" SAR and computational analysis.

While most analogs that we have analyzed with changes in the structure of the "A-ring" were found to be either agonists or to have no activity, analogs with structural changes in the "C-ring" have both changes in potency and changes in function (agonism vs. antagonism). We first assessed the impact of the position of the nitro-substituent on the activity of the molecules (Table 3, entries 1-3), revealing the importance of an *ortho*-nitro substituent. We then prepared a series of analogs in which the *ortho*-nitro group on the "C-ring" of the parent compound (**3**) was exchanged for functionality that had been previously found to be a suitable bioisostere of an aromatic nitro group.[21] While the 2-pyridine was observed to have no agonist activity (entry 4) the di-fluoro bioisostere was found to show enhanced activity as a LasR agonist (entry 5). Introducing additional electron-withdrawing substituents onto the ring (entry 6) had minimal effect on activity however, interestingly, the pyrimidine analog (entry 7) was found to be active as an agonist. Combining the 2-nitro substitution with a ring nitrogen at the 4-position (entry 8) also provided an agonist of comparable activity to the parent compound. Therefore, within the series of aromatic and hetero-aromatic analogs of this ring highest agonist activity was noted with the di-fluoro analog (entry 5) and the 2-pyridine and *meta*- and *para*-nitro analogs were found to be inactive. Based on published crystal-structure analysis from which the *ortho*-nitro ring serves the role of a mimic of the homoserine lactone characteristic of this class of signaling molecules having direct interactions with a conserved tryptophan (W60) in the LasR binding pocket. Accordingly, we replaced the 2-nitro aniline "C-ring" with a homoserine lactone (**37**). Notably, this analog displays significantly enhanced activity to **3** and the native LasR signaling agonist, 3-oxo-C12-HSL, with an EC_{50} value of 0.9 nM (Entry 9).

3.3. Evaluation of the orientation of the central amide linker.

We next turned our attention to an evaluation of selected analogs identified as significant in our investigation of the SAR of Scaffold #2 as described in Tables 1 and 2. Accordingly we prepared a series of analogs based on Scaffold #1, maintaining the *ortho*-chloro substitutent on the "A-ring" and incorporating three selected "C-ring" motifs. We selected the new 2-pyridine, di-fluoro and pyrimidine "C-ring" analogs for this analysis as these analogs displayed a range of agonist activities in our initial library. Therefore, we evaluated analogs **32**, **33**, **35** and **38**-**40** for both their agonist and antagonist activity in the LasR quorum sensing reporter strain (Figure 4). In our analysis, we found that 2-pyridine analog **32**, earlier observed to show no agonist activity against LasR (Table 3, entry 4) possessed potent antagonist activity with an IC_{50} of 42μM. We additionally prepared this analog with the amide linker between the "B-ring" and the "C-ring" reversed and observed that this analog (**38**) had similarly high LasR antagonist activity (Figure 4). We next prepared an

Table 3. Structure-activity relationships of "C-ring" analogs.

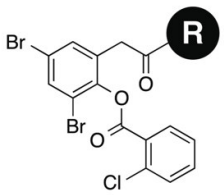

Entry	Structure	EC_{50} (μM)[a]	% Max[b]
1	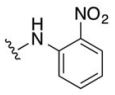 **3**	0.372±0.041	105
2	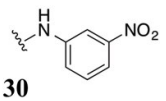 **30**	<50.0	0
3	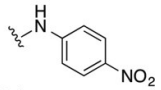 **31**	<50.0	0
4	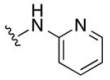 **32**	<50.0	0
5	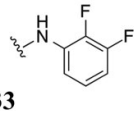 **33**	0.0456± 0.0038	116
6	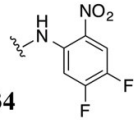 **34**	0.335±0.194	89
7	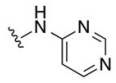 **35**	0.601±0.464	92
8	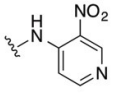 **36**	0.446±0.257	112
9	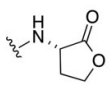 **37**	0.000896± 0.0021	105

[a] EC_{50} values are reported as the mean of triplicate analysis with the range defining the standard deviation. The native LasR agonist (**1**) was used as a control with an EC_{50}=72.9±24.6nM. [b] Maximal percent activation of GFP at 50 μM with respect to 3-oxo-C12 HSL (**1**) as a positive control for LasR agonism, set at 100% activation.

analog containing a reversed amide corresponding to the potent difluoro arene full LasR agonist **33** (Figure 4, EC_{50} = 46nM). To

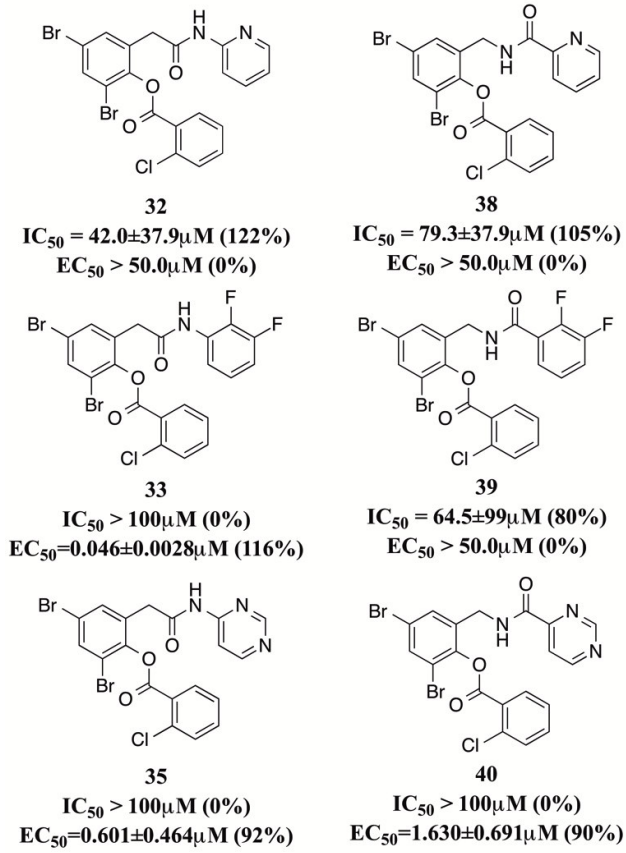

Figure 4. The effect of amide bond orientation on the activity of selected LasR ligands. Bioassay and data fitting was performed according to the standard procedure. EC_{50} and IC_{50} values are reported as the mean of triplicate analysis with the range defining the standard deviation.

our surprise, the analog containing the reversed amide as in Scaffold #1 (**39**) was not an agonist of LasR, instead it displayed a change in *function*, instead acting as an partial antagonist of LasR QS with an IC_{50} of 65uM (80% maximal inhibition). In contrast to this finding, when we prepared the reversed amide analog of the weak agonist pyrimidine **34** (EC_{50} = 0.6μM) we found the new analog (**40**) to similarly be a weak agonist of LasR with an EC_{50} of 1.6 μM. Therefore, while in most cases we evaluated changing the orientation of the amide linker results in small (2-3 fold) changes in the potency of the analog, in certain cases simply reversing this amide linkage appears to result in a shift from LasR agonism to antagonism.

We turned to computational modeling in an effort to further investigate these observations. In contrast to the ligands in Table 1, where a clear binding preference was noted for *ortho*-substituted "A-ring" analogs based on MMGBSA scores, in this analysis the ligands shown in Figure 5 are universally predicted to have show comparable binding to LasR. As before, we therefore evaluated the independent contributions of amino acid residues within the LasR binding pocket (Figure 5). Importantly, all of the residues that are proximal to the "A-ring" and "B-ring", which are unchanged in this series of ligands show minimal changes in their binding energies (e.g. Y47, R61, D65, V76, G126 and A127, Figure 5). One significant change in binding energies at the individual amino acid level is noted and occurs with a residue predicted to be close to the "C-ring" of the ligand. The pyridine analog **32**, an antagonist, shows a stronger binding interaction with Y56 along with diminished binding to W60 when compared to **3** and **33**, two agonists. Evaluation of the docking poses for these ligands reveals a notable reorganization of the ligand which likely leads to the above changes in the binding energies for Y56 and W60 (Figure 6). In these poses there is a clear shift in protein binding involving rotation of the "C-ring" from interaction between the 2-nitro substituent of the agonist **3** with W60 (light blue, Figure 6A) to an interaction between the 2-pyridine of the antagoinst **32** with Y56 (yellow, Figure 6B).

Figure 5. Computational binding contributions of individual amino acids in LasR with agonist ligands **3** (dark grey) and **33** (light grey) and the antagonist ligand **32** (medium grey).

We hypothesized that this subtle change in protein binding may represent a novel trigger to shift LasR from an agonized to an antagonized state. To test this hypothesis we prepared an analog containing a 3-pyridine ring in leiu of the 2-pyridine ring contained in the antagonist **32**. Due to the placement of the ring nitrogen, the pyridine should be prevented from interacting with Y56 and we hypothesized would therefore lose its antagonist activity. We accordingly evaluated **41** (Figure 7) and found this analog to show no antagonist activity, in striking contrast to the 2-pyridine antagonist (**32**), this analog acts as an agonist of LasR.

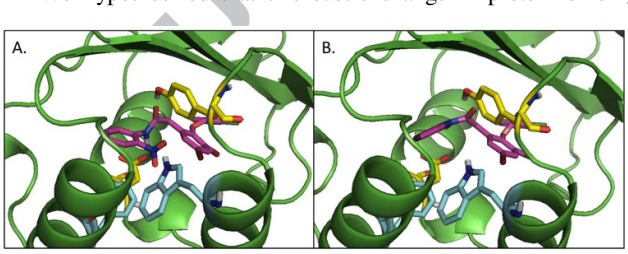

Figure 6. Comparison of the docking poses for LasR agonist **3** (panel A) and LasR antagonist **32** (panel B).

We had previously identified a novel series of potent maleimide containing LasR antagoinsts that act to irreversibly inhibit LasR through covalent modification of Cys79 in the LasR binding pocket.[22] Structurally, the maleimide functionality we identified as being central to the LasR antagonist activity maps onto the "A-ring" of the current ligand series. Accordingly we investigated a series of hybrid analogs containing a 2-pyridine or a homoseriene lactone in the "C-ring" position and a pendant

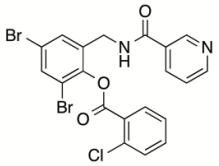

Figure 7. The 3-pyridine analog is a LasR agonist. Bioassay and data fitting was performed according to the standard procedure. EC_{50} and IC_{50} values are reported as the mean of triplicate analysis with the range defining the standard deviation.

maleimide as the "A-ring" structure (Figure 9). Upon analysis of this series of compounds we found that all fully antagonized LasR, however with considerably different levels of activity (Figure 9). Analog **42**, combining the 2-pyridine "C-ring" with a pendant maleimide was found to be a weak antagonist of LasR. It appears that combining the two structural features we had identified to independently lead to LasR antagonism, through two distinct mechanisms of interaction with LasR, do not work together in this ligand in an additive manner. Analogs **43** and **44** both containing a homoseriene lactone in place of the 2-nitro aniline "C-ring" display a striking dependence of activity on the linker length to the maleimide. Consistent with our previous studies for ligands containing this amide isomer[22], the maleimide linker containing two methylene units (**44**) was more potent with an IC_{50} of 23.8μM. This analog represents one of the most potent antagonists of LasR discovered, being comparable in activity to the most potent analogs we had previously identified.[22]

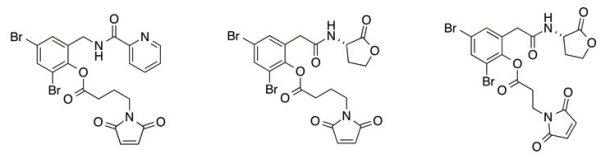

Figure 8. Hybrid analogs combining optimized structural features identified in this study with a maleimide for LasR irreversible inhibition. Bioassay and data fitting was performed according to the standard procedure. EC_{50} and IC_{50} values are reported as the mean of triplicate analysis with the range defining the standard deviation.

4. Conclusions.

We have evaluated a series of synthetic libraries of non-natural modulators of LasR-mediated QS in *P. aeruginosa*. The compounds prepared are significant as they represent a novel drug-like scaffold for the preparation of inhibitors of bacterial virulence. We have identified several notable stricture-activity relationships and in so doing have paved the way for the rational design of potent drug-like inhibitors of LasR QS. Using a combination of experimental and computational investigations, our studies have unveiled a new potential strategy for inducing LasR antagonism and have defined critical structural features of this novel ligand class for receptor binding.

5. Experimental section.

5.1. Chemistry

5.1.1. General Experimental.

Unless otherwise noted, all reactions were performed in flame-dried glassware under an atmosphere of nitrogen or argon using dried reagents and solvents. All chemicals were purchased from commercial vendors and used without further purification. Anhydrous solvents were purchased from commercial vendors.

Flash chromatography was performed using standard grade silica gel 60 230-400 mesh from SORBENT Technologies or was performed using a Biotage Flash Purification system equipped with Biotage SNAP columns. All purifications were performed using gradients of mixtures of ethyl acetate and hexanes. Analytical thin-layer chromatography was carried out using Silica G TLC plates, 200 μm with UV_{254} fluorescent indicator (SORBENT Technologies), and visualization was performed by staining and/or by absorbance of UV light.

NMR spectra were recorded using a Varian Mercury Plus spectrometer (400 MHz for ^{1}H-NMR; 100 MHz for ^{13}C-NMR). Chemical shifts are reported in parts per million (ppm) and were calibrated according to residual protonated solvent. Mass spectroscopy data was collected using an Agilent 1100-Series LC/MSD Trap LC-MS or a Micromass Quattromicro with a Waters 2795 Separations Module LC-MS with acetonitrile containing 0.1% formic acid as the mobile phase in positive ionization mode. Purity was determined on a Agilent 1100 series equipped with a Phenomenex Kinetex 2.6 μm C18-UPLC column using a gradient of water to acetonitrile with 0.1% TFA.

All final compounds were evaluated to be of greater then 90% purity by analysis of ^{1}H-NMR, ^{13}C-NMR, and analytical HPLC. Full ^{1}H-NMR and ^{13}C-NMR spectra are included in the online supporting information.

5.1.2. 2-(Benzyloxy)-3,5-dibromobenzamide, ***10****.*

Salicylamide (10.0 g, 72.9 mmol) was dissolved in glacial acetic acid (146 mL, 0.5 M) and Br_2 (11.2 mL, 218.7 mmol) was added dropwise. The reaction stirred overnight at room temperature and then was quenched with water (500 mL). Product was filtered and washed with a small amount of water and then dried in a dessicator, affording 20.2 g of the desired product, which was used crude in the subsequent step, 93.5% yield. 3,5-Dibromo-2-hydroxybenzamide (10.0 g, 33.7 mmol) was dissolved in acetone (337 mL, 0.1 M) and K_2CO_3 (5.58 g, 40.4 mmol) was added, followed by benzyl bromide (4.80 mL, 40.4 mmol) dropwise. The mixture was stirred at reflux overnight and then was cooled to room temperature. Potassium carbonate was filtered off (filtrate was washed with more acetone) and the solvent was removed in vacuo. The product was recrystallized in acetone, affording 11.3 g of the desired product, 87.1% yield. Spectral data was consistent with previous report.[22]

5.1.3. N-(2-(Benzyloxy)-3,5-dibromobenzyl)-2-nitrobenzamide, ***12****.*

2-(Benzyloxy)-3,5-dibromobenzamide (1.0 g, 2.58 mmol) was dissolved in BH_3·THF (13.24 mL, 13.24 mmol) under N_2 and the mixture was heated to reflux. The reaction stirred for 48 h at 75 °C and was monitored by TLC (10 mL additional BH_3·THF was added at 30 h). Methanol (10 mL x 2) was added dropwise to quench the reaction, and then the solvent was removed in vacuo. The product was used crude in the subsequent step without purification. ^{1}H NMR (400 MHz, DMSO-d_6) δ 7.95 (d, J = 2.5 Hz, 1H), 7.91 (s, 1H), 7.74 (s, 1H), 7.60 (d, J = 2.4 Hz, 1H), 7.48 – 7.42 (m, 2H), 7.40 – 7.29 (m, 3H), 4.95 (s, 2H), 4.36 (t, 2H). ^{13}C NMR (101 MHz, DMSO-d_6) δ 151.79, 136.32, 136.20, 134.68, 131.19, 128.40, 128.39, 119.03, 116.67, 60.79, 29.25. 2-Nitrobenzonic acid (534.8 mg, 3.20 mmol) was dissolved in CH_2Cl_2 and the solution was cooled to 0 °C under N_2. Oxalyl chloride (0.550 mL, 6.40 mmol) was added dropwise, followed by DMF (1 drop). The reaction was allowed to warm to room temperature as it stirred for 2 h. Solvent and excess oxalyl chloride was removed in vacuo and then the residue was resuspended in CH_2Cl_2. This acid chloride was added dropwise to a solution of (2-(benzyloxy)-3,5-dibromophenyl)methanamine (655 mg, 1.60 mmol) in CH_2Cl_2 (32 mL, 0.1 M). Triethylamine (1.56 mL, 11.2 mmol) was added, followed by DMAP (cat.) and the mixture stirred overnight at room temperature. After quenching the reaction with water (25 mL), more CH_2Cl_2 was added (50 mL) and the organic layer was washed with HCl (50 mL, 1 M), sat. $NaHCO_3$ (50 mL) and then brine (50 mL), and then was dried over Na_2SO_4. Purification via silica-gel column chromatography (product elutes around 30% EtOAc) afforded 354 mg of the desired product, 42.5% yield. ^{1}H NMR (400 MHz, $CDCl_3$) δ 8.04 (dd, 1H), 7.69 (d, J = 2.4 Hz, 1H), 7.66 – 7.59 (m,

1H), 7.59 – 7.53 (m, 2H), 7.44 – 7.40 (m, 2H), 7.37 – 7.29 (m, 3H), 7.26 – 7.20 (m, 1H), 5.81 (t, *J* = 6.1 Hz, 1H), 5.05 (s, 2H), 4.46 (d, *J* = 6.1 Hz, 2H). ^{13}C NMR (101 MHz, $CDCl_3$) δ 166.46, 153.03, 146.43, 136.07, 135.70, 134.99, 133.83, 132.54, 132.45, 130.73, 129.03, 128.89, 128.87, 128.75, 124.72, 118.29, 117.99, 75.85, 39.21.

5.1.4. 2,4-Dibromo-6-((2-nitrobenzamido)methyl)phenyl 2-chlorobenzoate, ***2****.*

N-(2-(Methoxy)-3,5-dibromobenzyl)-2-nitrobenzamide (354 mg, 0.681 mmol) was dissolved in CH_2Cl_2 (4.54 mL, 0.15 M) and cooled to -78 °C in a dry ice/acetone bath. BBr_3 (65 µL, 0.681 mmol) was added dropwise and the mixture stirred for 3 h while the temperature was kept between -20 and -60 °C. The reaction was quenched with sat. $NaHCO_3$ (25 mL) and was extracted with CH_2Cl_2 (50 mL). This organic layer was washed with brine and then dried over Na_2SO_4. Purification via silica-gel column chromatography (product elutes around 40% EtOAc) afforded 129.5 mg of the desired product, 30.2% yield. ^{1}H NMR (400 MHz, DMSO-d_6) δ 9.25 (t, *J* = 6.2 Hz, 1H), 7.99 (d, *J* = 8.0 Hz, 1H), 7.75 (t, *J* = 7.5 Hz, 1H), 7.70 – 7.56 (m, 3H), 7.34 (d, *J* = 2.2 Hz, 1H), 4.37 (d, *J* = 5.1 Hz, 2H). ^{13}C NMR (101 MHz, DMSO-d_6) δ 166.33, 151.20, 147.18, 133.78, 133.02, 131.85, 131.14, 130.27, 130.03, 129.20, 124.28, 112.36, 110.97, 38.51. ESI-MS calculated for $C_{14}H_{11}Br_2N_2O_4$ 428.9 [M+H], observed 428.9. This product was reacted with 2-chlorobenzoyl chloride following the procedure for 2,4-dibromo-6-(2-((2-nitrophenyl)amino)-2-oxoethyl)phenyl 2-chlorobenzoate to provide the desired product, 72.1 mg (92% yield). Spectral data was consistent with previous report.[19]

5.1.5. 2,4-Dibromo-6-(2-((2-nitrophenyl)amino)-2-oxoethyl)phenyl 2-chlorobenzoate, ***3****.*

To 2-(3,5-dibromo-2-hydroxyphenyl)-*N*-(2-nitrophenyl)acetamide[22] (53.0 mg, 0.123 mmol) in CH_2Cl_2 (2.46 mL, 0.05 M) under N_2 was added 2-chlorobenzoyl chloride (19 µL, 0.148 mmol), followed by Et_3N (41 µL, 0.295 mmol) and then DMAP (1.5 mg, 0.0123 mmol). The mixture was allowed to stir overnight at room temperature and then was diluted with CH_2Cl_2 (50 mL) and washed with HCl (25 mL, 1 M), sat. $NaHCO_3$ (25 mL) and then brine (25 mL). After drying over Na_2SO_4, the material was purified via silica-gel flash chromatography, affording 12.4 mg of the desired product (55% yield). ^{1}H-NMR (500MHz, $CDCl_3$) δ 10.32 (s, 1H), 8.67 (dd, *J* = 8.5, 1.1 Hz, 1H), 8.17-8.10 (m, 2H), 7.81 (d, *J* = 2.2 Hz, 1H), 7.63-7.56 (m, 2H), 7.50-7.45 (m, 2H), 7.36-7.30 (m, 1H), 7.16 (ddd, *J* = 8.5, 7.3, 1.3 Hz, 1H), 3.78 (s, 2H). ^{13}C-NMR (125MHz, $CDCl_3$) δ 169.8, 162.2, 146.6, 136.6, 136.2, 135.9, 135.1, 134.5, 134.2, 133.8, 132.6, 131.7, 130.7, 127.6, 127.1, 125.9, 123.9, 122.4, 120.6, 118.9, 40.8. ESI-MS calculated for $C_{21}H_{14}Br_2ClN_2O_5$, 566.89 [M+H], observed 566.82. HPLC purity 90.1%.

5.1.6. 2,4-Dibromo-6-(2-((2-nitrophenyl)amino)-2-oxoethyl)phenyl 3-chlorobenzoate, ***13****.*

Prepared according to the procedure provided for 2,4-dibromo-6-(2-((2-nitrophenyl)amino)-2-oxoethyl)phenyl 2-chlorobenzoate using the appropriate acid chloride, affording 11.7 mg of the desired product (52% yield). ^{1}H-NMR (500MHz, $CDCl_3$) δ 10.35 (s, 1H), 8.68 (d, *J* = 8.4 Hz, 1H), 8.15 (dd, *J* = 8.5, 1.3 Hz, 1H), 8.09-8.05 (m, 1H), 8.02 (d, *J* = 7.9 Hz, 1H), 7.79 (d, *J* = 2.2Hz, 1H), 7.63 (ddd, *J* = 8.5, 7.2, 1.0 Hz, 1H), 7.60-7.54 (m, 2H), 7.39 (t, *J* = 7.9 Hz, 1H), 7.18 (ddd, *J* = 8.4, 7.3, 1.1 Hz, 1H), 3.71 (s, 2H). ^{13}C-NMR (125MHz, $CDCl_3$) δ 167.8, 162.6, 146.6, 136.4, 136.3, 135.8, 135.2, 134.6, 134.5, 133.8, 130.8, 130.6, 130.3, 129.7, 128.8, 126.0, 123.9, 122.2, 120.6, 118.8, 41.0. ESI-MS calculated for $C_{21}H_{14}Br_2ClN_2O_5$, 566.89 [M+H], observed 566.90. HPLC purity 92.2%.

5.1.7. 2,4-Dibromo-6-(2-((2-nitrophenyl)amino)-2-oxoethyl)phenyl 4-chlorobenzoate, ***14****.*

Prepared according to the procedure provided for 2,4-dibromo-6-(2-((2-nitrophenyl)amino)-2-oxoethyl)phenyl 2-chlorobenzoate using the appropriate acid chloride, affording 15.8 mg of the desired product (70% yield). ^{1}H-NMR (500MHz, $CDCl_3$) δ 10.33 (s, 1H), 8.67 (dd, *J* = 8.5, 1.1 Hz, 1H), 8.15 (dd, *J* = 8.5, 1.5 Hz, 1H), 8.08-8.03 (m, 2H), 7.79 (d, *J* = 2.2 Hz, 1H), 7.62 (ddd, *J* = 8.6, 7.2, 1.4 Hz, 1H), 7.57 (d, *J* = 2.2 Hz, 1H), 7.43-7.37 (m, 2H), 7.18 (ddd, *J* = 8.5, 7.2, 1.2 Hz, 1H), 3.71 (s, 3H). ^{13}C-NMR (125MHz, $CDCl_3$) δ 167.9, 163.0, 146.7, 141.2, 136.4, 136.2, 135.8, 134.5, 133.7, 132.0, 130.8, 129.4, 126.4, 126.0, 123.9, 122.2, 120.5, 118.8, 41.0. ESI-MS calculated for $C_{21}H_{14}Br_2ClN_2O_5$, 566.89 [M+H], observed 566.80. HPLC purity 91.7%.

5.1.8. 2,4-Dibromo-6-(2-((2-nitrophenyl)amino)-2-oxoethyl)phenyl 2-bromobenzoate, ***15****.*

Prepared according to the procedure provided for 2,4-dibromo-6-(2-((2-nitrophenyl)amino)-2-oxoethyl)phenyl 2-chlorobenzoate using the appropriate acid chloride, affording 14.3 mg of the desired product (63% yield). ^{1}H-NMR (500MHz, $CDCl_3$) δ 10.32 (s, 1H), 8.68 (dd, *J* = 8.5, 1.0 Hz, 1H), 8.17-8.11 (m, 2H), 7.81 (d, *J* = 2.2 Hz, 1H), 7.71-7.66 (m, 1H), 7.63-7.57 (m, 2H), 7.41-7.36 (m, 2H), 7.16 (ddd, *J* = 8.5, 7.2, 1.2 Hz, 1H), 3.79 (s, 2H). ^{13}C-NMR (125MHz, $CDCl_3$) δ 167.8, 162.7, 146.6, 136.6, 136.1, 135.9, 135.1, 134.5, 134.1, 133.8, 132.7, 130.7, 129.5, 127.6, 126.0, 123.9, 123.1, 122.4, 120.6, 118.8, 40.8. ESI-MS calculated for $C_{21}H_{14}Br_3N_2O_5$, 610.84 [M+H], observed 610.79. HPLC purity 91.2%.

5.1.9. 2,4-Dibromo-6-(2-((2-nitrophenyl)amino)-2-oxoethyl)phenyl 3-bromobenzoate, ***16****.*

Prepared according to the procedure provided for 2,4-dibromo-6-(2-((2-nitrophenyl)amino)-2-oxoethyl)phenyl 2-chlorobenzoate using the appropriate acid chloride, affording 16.3 mg of the desired product (67% yield). ^{1}H-NMR (500MHz, $CDCl_3$) δ 10.35 (s, 1H), 8.68 (dd, *J* = 8.5, 1.0 Hz, 1H), 8.22 (t, *J* = 1.0 Hz, 1H), 8.15 (dd, *J* = 8.4, 1.0 Hz, 1H), 8.06 (d, *J* = 8.5 Hz, 1H), 7.79 (d, *J* = 2.2 Hz, 1H), 7.75-7.71 (m, 1H), 7.64-7.61 (m, 1H), 7.57 (d, *J* = 2.1 Hz, 1H), 7.33 (t, *J* = 8.7 Hz, 1H), 7.18 (t, *J* = 8.6 Hz, 1H), 3.71 (s, 2H). ^{13}C-NMR (125MHz, $CDCl_3$) δ 167.8, 162.5, 146.6, 137.5, 136.3, 135.8, 134.5, 133.8, 133.5, 130.8, 130.5, 129.9, 129.3, 126.0, 124.0, 123.0, 122.2, 120.6, 118.7, 41.0. ESI-MS calculated for $C_{21}H_{14}Br_3N_2O_5$, 610.84 [M+H], observed 610.81. HPLC purity 98.1%.

5.1.10. 2,4-Dibromo-6-(2-((2-nitrophenyl)amino)-2-oxoethyl)phenyl 4-bromobenzoate, ***17****.*

Prepared according to the procedure provided for 2,4-dibromo-6-(2-((2-nitrophenyl)amino)-2-oxoethyl)phenyl 2-chlorobenzoate using the appropriate acid chloride, affording 15.1 mg of the desired product (62% yield). ^{1}H-NMR (500MHz, $CDCl_3$) δ 10.34 (s, 1H), 8.68 (dd, *J* = 8.5, 0.9 Hz, 1H), 8.16 (dd, *J* = 8.4, 1.0 Hz, 1H), 7.98 (d, *J* = 8.5 Hz), 7.79 (d, *J* = 2.3 Hz, 1H), 7.65-7.54 (m, 3H), 7.18 (t, *J* = 8.4 Hz, 1H), 3.71 (s, 2H). ^{13}C-NMR (125MHz, $CDCl_3$) δ 167.9, 163.1, 146.7, 136.3, 135.8, 134.5, 133.7, 132.4, 132.1, 130.8, 130.0, 126.8, 126.0, 123.9, 122.2, 120.6, 118.8, 41.0. ESI-MS calculated for $C_{21}H_{14}Br_3N_2O_5$, 610.84 [M+H], observed 610.82. HPLC purity 93.6%.

5.1.11. 2,4-Dibromo-6-(2-((2-nitrophenyl)amino)-2-oxoethyl)phenyl 2-fluorobenzoate, ***18****.*

Prepared according to the procedure provided for 2,4-dibromo-6-(2-((2-nitrophenyl)amino)-2-oxoethyl)phenyl 2-chlorobenzoate

using the appropriate acid chloride, affording 15.4 mg of the desired product (70% yield). ^{1}H-NMR (500MHz, $CDCl_3$) δ 10.32 (s, 1H), 8.67 (dd, *J* = 8.4, 0.9 Hz, 1H), 8.15 (dd, *J* = 8.5, 1.0 Hz, 1H), 8.06 (dt, *J* = 8.4, 0.9 Hz, 1H), 7.79 (d, *J* = 2.2 Hz, 1H), 7.64-7.55 (m, 2H), 7.24-7.11 (m,2H), 3.75 (s, 2H). ^{13}C-NMR (125MHz, $CDCl_3$) δ167.8, 163.7, 161.6, 161.2, 161.1, 136.3, 136.2, 136.2, 135.8, 134.5, 133.7, 133.0, 130.7, 125.9, 124.5, 124.5, 123.9, 122.4, 120.5, 118.8, 117.6, 117.4, 116.7, 116.6, 40.8. ESI-MS calculated for $C_{21}H_{14}Br_2FN_2O_5$, 550.93 [M+H], observed 550.91. HPLC purity 95.8%.

5.1.12. 2,4-Dibromo-6-(2-((2-nitrophenyl)amino)-2-oxoethyl)phenyl 4-fluorobenzoate, ***19***.

Prepared according to the procedure provided for 2,4-dibromo-6-(2-((2-nitrophenyl)amino)-2-oxoethyl)phenyl 2-chlorobenzoate using the appropriate acid chloride, affording 12.7 mg of the desired product (58% yield). ^{1}H-NMR (500MHz, $CDCl_3$) δ 10.33 (s, 1H), 8.67 (d, *J* = 8.3 Hz, 1H), 8.20-8.11 (m, 2H), 7.79 (d, *J* = 1.9 Hz, 1H), 7.62 (t, *J* = 8.4 Hz, 1H), 7.57 (d, *J* = 1.8 Hz, 1H), 7.18 (t, *J* = 8.4 Hz, 1H), 7.14-7.07 (m, 2H), 3.71 (s, 2H). ^{13}C-NMR (125MHz, $CDCl_3$) δ167.9, 167.8, 165.7, 162.8, 146.7, 136.5, 136.2, 135.7, 134.5, 133.7, 133.5, 133.4, 130.8, 126.0, 124.2, 123.9, 122.2, 120.5, 118.8, 116.4, 116.2, 40.9. ESI-MS calculated for $C_{21}H_{14}Br_2FN_2O_5$, 550.93 [M+H], observed 550.90. HPLC purity 92.0%.

5.1.13. 2,4-Dibromo-6-(2-((2-nitrophenyl)amino)-2-oxoethyl)phenyl 2-iodobenzoate, ***20***.

Prepared according to the procedure provided for 2,4-dibromo-6-(2-((2-nitrophenyl)amino)-2-oxoethyl)phenyl 2-chlorobenzoate using the appropriate acid chloride, affording 9.5 mg of the desired product (77% yield). ^{1}H NMR (400 MHz, $CDCl_3$) δ 10.33 (s, 1H), 8.70 (dt, *J* = 8.5, 1.2 Hz, 1H), 8.23 – 8.13 (m, 2H), 8.05 (dt, *J* = 7.9, 1.2 Hz, 1H), 7.82 (dd, *J* = 2.4, 1.1 Hz, 1H), 7.65 – 7.57 (m, 2H), 7.47 – 7.39 (m, 1H), 7.26 – 7.13 (m, 2H), 3.80 (d, *J* = 1.0 Hz, 2H). ^{13}C NMR (101 MHz, $CDCl_3$) δ 167.72, 162.75, 142.23, 141.98, 136.02, 135.78, 135.03, 134.46, 134.11, 133.74, 132.34, 132.11, 130.68, 129.74, 128.30, 125.88, 123.80, 122.38, 120.54, 118.79, 40.81. ESI-MS calculated for $C_{21}H_{14}Br_2IN_2O_5$, 658.83 [M+H], observed 658.90. HPLC purity 96.8%.

5.1.14. 2,4-Dibromo-6-(2-((2-nitrophenyl)amino)-2-oxoethyl)phenyl 2-methylbenzoate, ***21***.

Prepared according to the procedure provided for 2,4-dibromo-6-(2-((2-nitrophenyl)amino)-2-oxoethyl)phenyl 2-chlorobenzoate using the appropriate acid chloride, affording 16.0 mg of the desired product (61% yield). ^{1}H-NMR (500MHz, $CDCl_3$) δ 10.33 (s, 1H), 8.68 (d, *J* = 8.4 Hz, 1H), 8.16 (d, *J* = 8.4 Hz, 1H), 8.13 (dd, *J* = 8.4, 0.9 Hz, 1H), 7.80 (d, *J* = 2.0 Hz, 1H), 7.60 (t, *J* = 8.2 Hz, 1H), 7.57 (d, *J* = 1.9 Hz, 1H), 7.44 (t, *J* = 8.2 Hz, 1H), 7.27-7.13 (m, 2H), 3.73 (s, 2H), 2.53 (s, 3H). ^{13}C-NMR (125MHz, $CDCl_3$) δ168.0, 163.9, 147.0, 142.4, 136.5, 136.1, 135.7, 134.5, 133.7, 133.7, 132.3, 131.8, 130.9, 126.8, 126.2, 125.9, 123.8, 122.2, 120.2, 119.1, 41.0, 22.1. ESI-MS calculated for $C_{22}H_{17}Br_2N_2O_5$, 546.95 [M+H], observed 546.89. HPLC purity 96.4%.

5.1.15. 2,4-Dibromo-6-(2-((2-nitrophenyl)amino)-2-oxoethyl)phenyl 3-methylbenzoate, ***22***.

Prepared according to the procedure provided for 2,4-dibromo-6-(2-((2-nitrophenyl)amino)-2-oxoethyl)phenyl 2-chlorobenzoate using the appropriate acid chloride, affording 15.8 mg of the desired product (72% yield). ^{1}H-NMR (500MHz, $CDCl_3$) δ 10.33 (s, 1H), 8.70 (dd, *J* = 8.4, 0.8 Hz, 1H), 8.13 (dd, *J* = 8.4, 0.9 Hz), 7.94-7.89 (m, 2H), 7.78 (d, *J* = 2.1, Hz, 1H), 7.61 (t, *J* = 8.2 Hz, 1H), 7.56 (d, *J* = 2.1 Hz, 1H), 7.43-7.37 (m, 1H), 7.30 (t, *J* = 8.4 Hz, 1H), 7.16 (t, *J* = 8.4 Hz, 1H), 3.71 (s, 2H), 2.33 (s, 3H). ^{13}C-NMR (125MHz, $CDCl_3$) δ 167.9, 163.9, 146.9, 138.9, 136.4, 136.2, 135.7, 135.4, 134.6, 133.7, 131.1, 130.9, 128.8, 127.9, 127.8, 125.9, 123.8, 122.2, 120.3, 118.9, 40.9, 21.4. ESI-MS calculated for $C_{22}H_{17}Br_2N_2O_5$, 546.95 [M+H], observed 546.96. HPLC purity 94.4%.

5.1.16. 2,4-Dibromo-6-(2-((2-nitrophenyl)amino)-2-oxoethyl)phenyl 4-methylbenzoate, ***23***.

Prepared according to the procedure provided for 2,4-dibromo-6-(2-((2-nitrophenyl)amino)-2-oxoethyl)phenyl 2-chlorobenzoate using the appropriate acid chloride, affording 17.1 mg of the desired product (78% yield). ^{1}H-NMR (500MHz, $CDCl_3$) δ 10.32 (s, 1H), 8.69 (dd, *J* = 8.4, 0.9 Hz, 1H), 8.13 (dd, *J* = 8.4, 0.9 Hz, 1H), 8.00 (d, *J* = 8.5 Hz, 2H), 7.78 (d, *J* = 2.1 Hz, 1H), 7.61 (t, *J* = 8.3 Hz, 1H), 7.56 (d, *J* = 2.1 Hz, 1H), 7.20 (d, *J* = 8.5 Hz, 2H), 7.17 (t, *J* = 8.4 Hz, 1H), 3.71 (s, 2H), 2.40 (s, 3H). ^{13}C-NMR (125MHz, $CDCl_3$) δ 168.0, 163.8, 146.9, 145.6, 136.4, 136.2, 135.7, 134.6, 133.6, 131.0, 130.8, 129.6, 125.9, 125.1, 123.8, 122.3, 120.2, 118.9, 40.9, 22.1. ESI-MS calculated for $C_{22}H_{17}Br_2N_2O_5$, 546.95 [M+H], observed 546.92. HPLC purity 91.7%.

5.1.17. 2,4-Dibromo-6-(2-((2-nitrophenyl)amino)-2-oxoethyl)phenyl 2-methoxybenzoate, ***24***.

Prepared according to the procedure provided for 2,4-dibromo-6-(2-((2-nitrophenyl)amino)-2-oxoethyl)phenyl 2-chlorobenzoate using the appropriate acid chloride, affording 10 mg of the desired product (65.6% yield). ^{1}H NMR (400 MHz, $CDCl_3$) δ 10.29 (s, 1H), 8.70 (dd, *J* = 8.5, 1.3 Hz, 1H), 8.15 (dd, *J* = 8.4, 1.6 Hz, 1H), 8.02 (dd, *J* = 7.8, 1.8 Hz, 1H), 7.80 (d, *J* = 2.3 Hz, 1H), 7.66 – 7.47 (m, 3H), 7.21 – 7.11 (m, 1H), 7.03 – 6.91 (m, 2H), 3.86 (s, 3H), 3.80 (s, 2H). ^{13}C NMR (101 MHz, $CDCl_3$) δ 168.09, 162.72, 160.18, 146.93, 136.61, 135.95, 135.60, 135.16, 134.51, 133.54, 132.69, 130.81, 125.82, 123.71, 122.36, 120.40, 120.06, 119.02, 117.52, 112.24, 56.10, 40.65. ESI-MS calculated for $C_{22}H_{17}Br_2N_2O_6$, 562.94 [M+H], observed 563.07. HPLC purity 89.9%.

5.1.18. 2,4-Dibromo-6-(2-((2-nitrophenyl)amino)-2-oxoethyl)phenyl 2-nitrobenzoate, ***25***.

Prepared according to the procedure provided for 2,4-dibromo-6-(2-((2-nitrophenyl)amino)-2-oxoethyl)phenyl 2-chlorobenzoate using the appropriate acid chloride, affording 14.4 mg of the desired product (19.1% yield). ^{1}H NMR (400 MHz, $CDCl_3$) δ 10.35 (s, 1H), 8.68 (dd, *J* = 8.6, 1.3 Hz, 1H), 8.13 (dd, *J* = 8.5, 1.2 Hz, 1H), 8.10 (dd, *J* = 7.4, 1.6 Hz, 1H), 8.01 (dd, *J* = 7.8, 1.4 Hz, 1H), 7.79 (d, 1H), 7.77 – 7.69 (m, 2H), 7.63 (d, 1H), 7.62 – 7.56 (m, 1H), 7.20 – 7.12 (m, 1H), 3.96 (s, 2H). ^{13}C NMR (101 MHz, $CDCl_3$) δ 167.90, 162.39, 147.98, 145.87, 136.78, 135.86, 135.52, 134.37, 134.16, 133.47, 132.80, 131.18, 130.53, 126.30, 125.74, 124.55, 123.71, 122.51, 120.82, 118.26, 39.85. ESI-MS calculated for $C_{21}H_{14}Br_2N_3O_7$, 577.92 [M+H], observed 577.79. HPLC purity 91.1%.

5.1.19. 2,4-Dibromo-6-(2-((2-nitrophenyl)amino)-2-oxoethyl)phenyl 2,6-dichlorobenzoate, ***27***.

Prepared according to the procedure provided for 2,4-dibromo-6-(2-((2-nitrophenyl)amino)-2-oxoethyl)phenyl 2-chlorobenzoate using the appropriate acid chloride, affording 18.6 mg of the desired product (78% yield). ^{1}H-NMR (500MHz, $CDCl_3$) δ 10.32 (s, 1H), 8.70 (d, *J* = 8.4 Hz, 1H), 8.16 (dd, *J* = 8.4, 1.0 Hz, 1H), 7.83 (d, *J* = 2.1 Hz, 1H), 7.64-7.57 (m, 2H), 7.41-7.31 (m, 2H), 7.16 (t, *J* = 8.4 Hz, 1H), 3.98 (s, 2H). ^{13}C-NMR (125MHz, $CDCl_3$) δ 167.9, 161.9, 146.1, 136.6, 136.3, 136.2, 134.5, 134.1, 133.0, 132.2, 131.2, 130.5, 128.9, 126.0, 123.9, 122.3, 121.1, 118.6, 40.5. ESI-MS calculated for $C_{21}H_{12}Br_2Cl_2N_2O_5$, 600.86 [M+H], observed 600.99. HPLC purity 91.2%.

5.1.20. 2-(3,5-Dibromo-2-((2,6-dichlorobenzyl)oxy)phenyl)-N-(2-nitrophenyl)acetamide, ***28***.

Prepared according to the procedure provided for 2,4-dibromo-6-(2-((2-nitrophenyl)amino)-2-oxoethyl)phenyl 2-chlorobenzoate using the appropriate acid chloride, affording 33.26 mg of the desired product (13.7% yield). ^{1}H NMR (400 MHz, $CDCl_3$) δ 10.13 (s, 1H), 8.62 (dd, *J* = 8.6, 1.3 Hz, 1H), 8.13 (dd, *J* = 8.5, 1.6 Hz, 1H), 7.68 (d, *J* = 2.4 Hz, 1H), 7.59 – 7.51 (m, 1H), 7.34 (d, *J* = 2.4 Hz, 1H), 7.25 – 7.21 (m, 2H), 7.17 – 7.07 (m, 2H), 5.45 (s, 2H), 3.54 (s, 2H). ^{13}C NMR (101 MHz, $CDCl_3$) δ 168.67, 153.71, 137.34, 136.56, 136.06, 135.91, 134.66, 133.49, 132.13, 131.17, 131.00, 128.81, 125.79, 123.52, 122.35, 118.51, 117.84, 70.16, 39.81. ESI-MS calculated for $C_{21}H_{15}Br_2Cl_2N_2O_4$, 586.87 [M+H], observed 586.76. HPLC purity 90.1%.

5.1.21. 2,4-Dibromo-6-(2-((2-nitrophenyl)amino)-2-oxoethyl)phenyl benzoate, ***29***.

Prepared according to the procedure provided for 2,4-dibromo-6-(2-((2-nitrophenyl)amino)-2-oxoethyl)phenyl 2-chlorobenzoate using the appropriate acid chloride, affording 7.3 mg of the desired product (62.1% yield). ^{1}H NMR (400 MHz, $CDCl_3$) δ 10.34 (s, 1H), 8.70 (dd, *J* = 8.5, 1.3 Hz, 1H), 8.18 – 8.12 (m, 3H), 7.81 (d, *J* = 2.2 Hz, 1H), 7.67 – 7.57 (m, 3H), 7.49 – 7.41 (m, 2H), 7.22 – 7.15 (m, 1H), 3.74 (s, 2H). ^{13}C NMR (101 MHz, $CDCl_3$) δ 167.85, 163.71, 136.07, 135.65, 134.50, 134.45, 133.57, 130.85, 130.64, 128.87, 127.94, 125.86, 123.76, 122.23, 120.28, 40.83. ESI-MS calculated for $C_{21}H_{14}Br_2N_2O_5$, 532.93 [M+H], observed 532.98. HPLC purity 90.0%.

5.1.22. 2,4-Dibromo-6-(2-((2-nitrophenyl)amino)-2-oxoethyl)phenyl 2-bromo-4-fluorobenzoate, ***26***.

Prepared according to the procedure provided for 2,4-dibromo-6-(2-((2-nitrophenyl)amino)-2-oxoethyl)phenyl 2-chlorobenzoate using the appropriate acid chloride, affording 9.5 mg of the desired product (11% yield). ^{1}H NMR (400 MHz, $CDCl_3$) δ 10.34 (s, 1H), 8.69 (dd, *J* = 8.5, 1.3 Hz, 1H), 8.17 (dd, *J* = 8.5, 1.5 Hz, 1H), 7.99 – 7.92 (m, 1H), 7.83 (d, *J* = 2.3 Hz, 1H), 7.63 – 7.58 (m, 2H), 7.45 – 7.30 (m, 2H), 7.22 – 7.15 (m, 1H), 3.81 (s, 2H). ^{13}C NMR (101 MHz, $CDCl_3$) δ 167.64, 161.84, 146.40, 138.59, 136.55, 136.08, 135.85, 134.37, 133.80, 131.53, 130.52, 128.88, 128.80, 127.94, 125.89, 123.88, 122.26, 120.84, 120.60, 118.68, 40.80. ESI-MS calculated for $C_{21}H_{12}Br_3FN_2O_5$, 628.84 [M+H], observed 629.18. HPLC purity 87.6%.

5.1.23. 2-(3,5-Dibromo-2-((2-chlorobenzoyl)oxy)phenyl)acetic acid.

To a solution of methyl 2-(3,5-dibromo-2-hydroxyphenyl)acetate (2.902g, 8.96mmol) in CH_2Cl_2 (59mL) at room temperature was added Et_3N (2.99mL, 21.49mmol), 2-chlorobenzoyl chloride (1.248g, 9.85mmol) and DMAP (0.109g, 0.896mmol). The mixture was allowed to react overnight and was diluted with CH_2Cl_2, quenched with 1M HCl, washed with sat. $NaHCO_3$ and brine, dried over Na_2SO_4, concentrated and purified by flash column chromatography to provide 2,4-dibromo-6-(2-methoxy-2-oxoethyl)phenyl 2-chlorobenzoate (2.91g, 70%). ^{1}H NMR (400 MHz, $CDCl_3$) δ 8.19-8.16 (m, 1H), 7.74 (d, J = 2.2 Hz, 1H), 7.56-7.72 (m, 2H), 7.50-7.48 (m, 1H), 7.44-7.39 (m, 1H), 3.64 (s, 3H), 3.62 (s, 2H). The above methyl ester, 2,4-dibromo-6-(2-methoxy-2-oxoethyl)phenyl 2-chlorobenzoate (1.823g, 3.94mmol) was dissolved in 1,2-dichloroethane (39.4mL) and was treated with trimethyltinhydroxide (1.425g, 7.88mmol). The mixture was heated to 80°C and was monitored by TLC to confirm the consumption of the starting material. After 2h the reaction was diluted with $CHCl_3$, washed with 1M HCl and sat. NaCl, dried over Na_2SO_4, concentrated and purified by flash column chromatography using a gradient of 20% EtOAc/hexanes to 100% EtOAc to provide 2-(3,5-dibromo-2-((2-chlorobenzoyl)oxy)phenyl)acetic acid as a white solid (1.045g, 59%). ^{1}H NMR (400 MHz, $CDCl_3$) δ 8.18-8.14 (m, 1H), 7.76 (d, *J* = 2.3 Hz, 1H), 7.55-7.52 (m, 2H), 7.50 (d, *J* = 2.2 Hz, 1H), 7.40 (ddd, *J* = 7.8, 5.6, 3.0 Hz, 1H), 3.65 (s, 2H).

5.1.24. 2,4-Dibromo-6-(2-((3-nitrophenyl)amino)-2-oxoethyl)phenyl 2-chlorobenzoate, ***30***.

To a solution of 2-(3,5-dibromo-2-((2-chlorobenzoyl)oxy)phenyl)acetic acid (0.181g, 0.4035mmol) in ACN (8.07mL) was added 3-nitroaniline (0.0613g, 0.4439mmol) followed by EDC (0.1423g, 0.807mmol) and DMAP (0.0049g, 0.0403mmol). The resulting mixture was allowed to react at room temperature overnight and was concentrated to dryness. The residue was suspended in $CHCl_3$, washed with 1M HCl, sat. $NaHCO_3$ and brine, dried over Na_2SO_4 and concentrated. The residue was purified by flash column chromatography using a gradient of hexanes to EtOAc, affording 1.1 mg of the desired product (0.5% yield). ^{1}H NMR (400 MHz, $CDCl_3$) δ 8.41 (t, *J* = 2.2 Hz, 1H), 8.26 (d, *J* = 7.4 Hz, 1H), 8.02 (s, 1H), 7.93 (d, *J* = 8.2 Hz, 1H), 7.86 (d, *J* = 8.1 Hz, 1H), 7.81 (d, *J* = 2.3 Hz, 1H), 7.62 (d, *J* = 2.3 Hz, 1H), 7.60 – 7.53 (m, 2H), 7.51 – 7.38 (m, 2H), 3.74 (s, 2H). ^{13}C NMR (101 MHz, $CDCl_3$) δ 167.29, 164.52, 148.63, 145.90, 138.97, 135.78, 135.38, 134.75, 133.24, 132.76, 131.92, 131.08, 129.80, 127.30, 127.00, 125.52, 121.07, 119.13, 118.63, 114.70, 39.55.. ESI-MS calculated for $C_{21}H_{14}Br_2ClN_2O_5$, 566.89 [M+H], observed 566.95. HPLC purity 91.3%.

5.1.25. 2,4-Dibromo-6-(2-((4-nitrophenyl)amino)-2-oxoethyl)phenyl 2-chlorobenzoate, ***31***.

Prepared according to the procedure provided for 2,4-dibromo-6-(2-((3-nitrophenyl)amino)-2-oxoethyl)phenyl 2-chlorobenzoate using the appropriate amine, affording 3.5 mg of the desired product (1.4% yield). ^{1}H NMR (400 MHz, $CDCl_3$) δ 8.26 (dd, *J* = 8.1, 1.5 Hz, 1H), 8.20 – 8.15 (m, 2H), 8.14 (s, 1H), 7.81 (d, *J* = 2.3 Hz, 1H), 7.74 – 7.67 (m, 2H), 7.64 – 7.54 (m, 3H), 7.50 – 7.42 (m, 1H), 3.74 (s, 2H). ^{13}C NMR (101 MHz, $CDCl_3$) δ 167.37, 164.71, 145.84, 143.77, 143.73, 135.85, 135.35, 134.81, 133.17, 132.76, 131.93, 130.93, 127.32, 127.00, 125.08, 121.14, 119.31, 118.63, 39.64. ESI-MS calculated for $C_{21}H_{14}Br_2ClN_2O_5$, 566.89 [M+H], observed 566.86. HPLC purity 94.8%.

5.1.26. 2,4-Dibromo-6-(2-oxo-2-(pyridin-2-ylamino)ethyl)phenyl 2-chlorobenzoate, ***32***.

Prepared according to the procedure provided for 2,4-dibromo-6-(2-((3-nitrophenyl)amino)-2-oxoethyl)phenyl 2-chlorobenzoate using the appropriate amine, affording 24.9 mg of the desired product (22% yield). ^{1}H NMR (400 MHz, $CDCl_3$) δ 8.27 – 8.19 (m, 2H), 8.19 – 8.10 (m, 2H), 7.77 (d, *J* = 2.3 Hz, 1H), 7.70 – 7.64 (m, 1H), 7.58 (d, *J* = 2.3 Hz, 1H), 7.53 – 7.48 (m, 2H), 7.40 – 7.32 (m, 1H), 7.05 – 6.99 (m, 1H), 3.73 (s, 2H). ^{13}C NMR (101 MHz, $CDCl_3$) δ 167.23, 162.64, 151.12, 147.96, 146.34, 138.49, 135.47, 135.01, 134.05, 133.44, 132.56, 131.66, 131.15, 127.73, 127.03, 120.48, 120.20, 118.56, 114.21, 39.73. ESI-MS calculated for $C_{20}H_{14}Br_2ClN_2O_3$, 522.91 [M+H], observed 522.97. HPLC purity 98.3%.

5.1.27. 2,4-Dibromo-6-(2-((2,3-difluorophenyl)amino)-2-oxoethyl)phenyl 2-chlorobenzoate, ***33***.

Prepared according to the procedure provided for 2,4-dibromo-6-(2-((3-nitrophenyl)amino)-2-oxoethyl)phenyl 2-chlorobenzoate using the appropriate amine, affording 24.9 mg of the desired product (41% yield). ^{1}H NMR (400 MHz, Acetone-d_6) δ 9.17 (s, 1H), 8.11 (dd, *J* = 7.9, 1.6 Hz, 1H), 7.80 (t, *J* = 7.4 Hz, 1H), 7.76 (d, *J* = 2.3 Hz, 1H), 7.65 (d, *J* = 2.3 Hz, 1H), 7.57 – 7.46 (m, 2H), 7.38 – 7.31 (m, 1H), 7.03 – 6.94 (m, 1H), 6.94 – 6.85 (m, 1H), 3.86 (s, 2H). ^{13}C NMR (101 MHz, $CDCl_3$) δ 167.08, 162.99,

146.01, 135.52, 135.05, 134.31, 133.18, 133.15, 132.57, 131.73, 131.12, 127.83, 127.46, 127.13, 124.21, 120.63, 118.48, 117.08, 112.62, 112.45, 39.66. ESI-MS calculated for $C_{21}H_{13}Br_2ClF_2NO_3$, 557.89 [M+H], observed 558.09. HPLC purity 92.3%.

5.1.28. 2,4-Dibromo-6-(2-((4,5-difluoro-2-nitrophenyl)amino)-2-oxoethyl)phenyl 2-chlorobenzoate, ***34***.

Prepared according to the procedure provided for 2,4-dibromo-6-(2-((3-nitrophenyl)amino)-2-oxoethyl)phenyl 2-chlorobenzoate using the appropriate amine, affording 36.7 mg of the desired product (16% yield). ^{1}H NMR (400 MHz, $CDCl_3$) δ 10.41 (s, 1H), 8.74 (dd, *J* = 12.6, 7.5 Hz, 1H), 8.14 (dd, *J* = 7.9, 0.9 Hz, 1H), 8.07 (dd, *J* = 10.1, 7.9 Hz, 1H), 7.85 (d, *J* = 2.3, 0.7 Hz, 1H), 7.59 (d, 1H), 7.55 – 7.49 (m, 2H), 7.41 – 7.35 (m, 1H), 3.81 (s, 2H). ^{13}C NMR (101 MHz, $CDCl_3$) δ 167.90, 162.12, 146.58, 136.02, 135.00, 134.18, 133.71, 132.55, 131.71, 130.14, 127.47, 127.05, 120.64, 118.93, 115.14, 114.93, 111.01, 110.76, 40.75. ESI-MS calculated for $C_{21}H_{12}Br_2ClN_3O_5$, 602.88 [M+H], observed 602.77. HPLC purity 97.0%.

5.1.29. 2,4-Dibromo-6-(2-oxo-2-(pyrimidin-4-ylamino)ethyl)phenyl 2-chlorobenzoate, ***35***.

Prepared according to the procedure provided for 2,4-dibromo-6-(2-((3-nitrophenyl)amino)-2-oxoethyl)phenyl 2-chlorobenzoate using the appropriate amine, affording 15.2 mg of the desired product (13% yield). ^{1}H NMR (400 MHz, $CDCl_3$) δ 8.83 (s, 1H), 8.61 (s, 1H), 8.34 (s, 1H), 8.21 – 8.14 (m, 1H), 8.10 (dd, *J* = 5.8, 1.2 Hz, 1H), 7.80 (d, *J* = 2.4 Hz, 1H), 7.57 (d, *J* = 2.4 Hz, 1H), 7.55 – 7.52 (m, 2H), 7.42 – 7.36 (m, 1H), 3.76 (s, 2H). ^{13}C NMR (101 MHz, $CDCl_3$) δ 168.19, 162.98, 158.59, 158.49, 156.87, 146.25, 135.79, 135.03, 134.27, 133.32, 132.57, 131.73, 130.43, 127.54, 127.12, 120.67, 118.71, 110.42, 39.79. ESI-MS calculated for $C_{19}H_{13}Br_2ClN_3O_3$, 523.90 [M+H], observed 523.92. HPLC purity 94.4%.

5.1.30. 2,4-Dibromo-6-(2-((3-nitropyridin-4-yl)amino)-2-oxoethyl)phenyl 2-chlorobenzoate, ***36***.

Prepared according to the procedure provided for 2,4-dibromo-6-(2-((3-nitrophenyl)amino)-2-oxoethyl)phenyl 2-chlorobenzoate using the appropriate amine, affording 4.1 mg of the desired product (5.8% yield). ^{1}H NMR (400 MHz, $CDCl_3$) δ 10.50 (s, 1H), 9.33 (s, 1H), 8.67 (s, 2H), 8.13 (dd, 1H), 7.86 (d, *J* = 2.2 Hz, 1H), 7.59 (d, *J* = 2.3 Hz, 1H), 7.56 – 7.47 (m, 2H), 7.41 – 7.34 (m, 1H), 3.84 (s, 2H). ^{13}C NMR (101 MHz, $CDCl_3$) δ 168.31, 162.10, 156.31, 155.69, 136.16, 134.22, 133.69, 132.54, 131.72, 129.85, 129.27, 128.07, 127.41, 127.06, 120.70, 118.99, 114.62, 40.90. ESI-MS calculated for $C_{20}H_{13}Br_2ClN_3O_5$, 567.89 [M+H], observed 567.82. HPLC purity 89.8%.

5.1.31. (S)-2,4-Dibromo-6-(2-oxo-2-((2-oxotetrahydrofuran-3-yl)amino)ethyl)phenyl 2-chlorobenzoate, ***37***.

Prepared according to the procedure provided for 2,4-dibromo-6-(2-((3-nitrophenyl)amino)-2-oxoethyl)phenyl 2-chlorobenzoate using the appropriate amine, affording 27.9 mg of the desired product (81% yield). ^{1}H NMR (400 MHz, $CDCl_3$) δ 8.21 (dd, *J* = 7.9, 1.2 Hz, 1H), 7.77 (dd, *J* = 2.3, 1.2 Hz, 1H), 7.59 – 7.53 (m, 3H), 7.47 – 7.40 (m, 1H), 6.18 (s, 1H), 4.55 – 4.35 (m, 2H), 4.29 – 4.14 (m, 1H), 3.61 (s, 2H), 2.76 – 2.61 (m, 1H), 2.16 – 1.99 (m, 1H). ^{13}C NMR (101 MHz, $CDCl_3$) δ 174.76, 169.16, 135.45, 135.02, 134.32, 133.47, 132.70, 131.78, 131.23, 127.48, 127.21, 120.57, 118.45, 66.07, 49.53, 38.19, 29.81. ESI-MS calculated for $C_{19}H_{15}Br_2ClNO_5$, 529.90 [M+H], observed 529.85. HPLC purity 94.9%.

5.1.32. 2,4-Dibromo-6-(picolinamidomethyl)phenyl 2-chlorobenzoate, ***38***.

The required phenol, *N*-(3,5-dibromo-2-hydroxybenzyl)picolinamide was prepared in two steps from (2-(benzyloxy)-3,5-dibromophenyl)methanamine and pyridine-2-carboxylic acid as described for N-(3,5-dibromo-2-hydroxybenzyl)-2-nitrobenzamide, providing the desired product (0.10g, 35%, two steps). ^{1}H NMR (400 MHz, Chloroform-d) δ 9.88 (s, 1H), 8.84 – 8.79 (m, 1H), 8.55 (d, J = 4.7 Hz, 1H), 8.20 (d, J = 7.8 Hz, 1H), 7.87 (dt, J = 7.7, 1.7 Hz, 1H), 7.59 (d, J = 2.4 Hz, 1H), 7.47 (ddd, J = 7.6, 4.7, 1.2 Hz, 1H), 7.29 (d, J = 2.4 Hz, 1H), 4.55 (d, J = 6.8 Hz, 2H). This product was reacted with 2-chlorobenzoyl chloride according to the procedure provided for 2,4-dibromo-6-((2 nitrobenzamido)methyl)phenyl 2-chlorobenzoate, affording 11.4 mg of the desired product (38% yield). ^{1}H NMR (400 MHz, $CDCl_3$) δ 8.54 (dd, *J* = 4.7, 1.4 Hz, 1H), 8.45 (s, 1H), 8.21 (dd, *J* = 7.8, 1.1 Hz, 1H), 8.15 (dd, *J* = 7.8, 1.1 Hz, 1H), 7.84 (td, *J* = 7.8, 1.8 Hz, 1H), 7.74 (d, *J* = 2.3 Hz, 1H), 7.58 (d, *J* = 2.3 Hz, 1H), 7.54 (d, 2H), 7.46 – 7.39 (m, 2H), 4.66 (d, *J* = 6.1 Hz, 2H). ^{13}C NMR (101 MHz, $CDCl_3$) δ 164.56, 162.48, 149.41, 148.35, 145.84, 137.52, 135.04, 134.94, 133.99, 132.61, 131.78, 131.65, 127.89, 127.00, 126.59, 122.51, 120.33, 118.12, 38.74. ESI-MS calculated for $C_{20}H_{14}Br_2ClN_2O_5$, 522.91 [M+H], observed 523.04. HPLC purity 97.7%.

5.1.33. 2,4-Dibromo-6-((2,3-difluorobenzamido)methyl)phenyl 2-chlorobenzoate, ***39***.

Prepared according to the procedure provided for 2,4-dibromo-6-((2 nitrobenzamido)methyl)phenyl 2-chlorobenzoate from 2-chlorobenzoyl chloride and *N*-(3,5-dibromo-2-hydroxybenzyl)-2,3-difluorobenzamide, affording 7.9 mg of the desired product (18% yield). ^{1}H NMR (400 MHz, $CDCl_3$) δ 8.21 (dd, 1H), 7.81 – 7.73 (m, 2H), 7.62 (d, *J* = 2.3 Hz, 1H), 7.57 – 7.53 (m, 2H), 7.46 – 7.40 (m, 1H), 7.36 – 7.27 (m, 1H), 7.21 – 7.14 (m, 1H), 7.04 (t, *J* = 11.4 Hz, 1H), 4.66 (s, 2H). ^{13}C NMR (101 MHz, $CDCl_3$) δ 162.73, 162.47, 145.94, 135.36, 134.98, 134.44, 134.12, 132.55, 132.25, 131.69, 127.75, 127.09, 126.60, 126.57, 124.78, 124.72, 120.83, 120.65, 120.43, 118.16, 39.40. ESI-MS calculated for $C_{21}H_{13}Br_2ClF_2NO_3$, 557.89 [M+H], observed 557.77. HPLC purity 90.0%.

5.1.34. 2,4-Dibromo-6-((pyrimidine-4-carboxamido)methyl)phenyl 2-chlorobenzoate, ***40***.

The required phenol, *N*-(3,5-dibromo-2-hydroxybenzyl)pyrimidine-4-carboxamide was prepared in two steps from (2-(benzyloxy)-3,5-dibromophenyl)methanamine and pyrimidine-4-carboxylic acid as described for N-(3,5-dibromo-2-hydroxybenzyl)-2-nitrobenzamide, providing the desired product (0.082g, 32%, two steps). ^{1}H-NMR (400 MHz, Chloroform-d) δ 9.22 (s, 1H), 8.99 (d, J = 5.0 Hz, 1H), 8.82 – 8.74 (m, 1H), 8.10 (dd, J = 5.0, 1.4 Hz, 1H), 7.56 (d, J = 2.4 Hz, 1H), 7.32 (d, J = 2.4 Hz, 1H), 4.59 (d, J = 6.7 Hz, 2H). This product was reacted with 2-chlorobenzoyl chloride according to the procedure provided for 2,4-dibromo-6-((2 nitrobenzamido)methyl)phenyl 2-chlorobenzoate, affording 7.7 mg of the desired product (7.0% yield). ^{1}H NMR (400 MHz, Chloroform-d) δ 9.22 (d, J = 1.4 Hz, 1H), 8.96 (d, J = 5.0 Hz, 1H), 8.38 (t, 1H), 8.20 (d, 1H), 8.06 (d, 1H), 7.76 (d, J = 2.3 Hz, 1H), 7.61 – 7.52 (m, 2H), 7.48 – 7.38 (m, 1H), 4.66 (d, J = 6.3 Hz, 2H). ^{13}C NMR (101 MHz, Chloroform-d) δ 162.91, 162.64, 159.41, 157.96, 155.96, 146.08, 135.49, 134.27, 134.21, 132.72, 132.17, 131.77, 127.84, 127.15, 126.84, 120.46, 118.87, 118.39, 39.10. ESI-MS calculated for $C_{19}H_{13}Br_2ClN_3O_3$, 523.90 [M+H], observed 523.67. HPLC purity 92.4%.

5.1.35. 2,4-Dibromo-6-(nicotinamidomethyl)phenyl 2-chlorobenzoate, ***41***.

The required phenol, *N*-(3,5-dibromo-2-hydroxybenzyl)nicotinamide was prepared in two steps from (2-(benzyloxy)-3,5-dibromophenyl)methanamine and nicotinic acid as described for N-(3,5-dibromo-2-hydroxybenzyl)-2-nitrobenzamide, providing the desired product (0.048g, 17%, two steps). ^{1}H-NMR (400 MHz, Chloroform-d) δ 9.03-8.91 (m, 1H), 8.81-8.71 (m, 1H), 8.15 (d, *J* = 8.1 Hz, 1H), 7.61 (d, *J* = 2.3 Hz, 1H), 7.42 (dd, *J* = 7.8, 5.0 Hz, 1H), 7.31 (d, *J* = 2.4 Hz, 1H), 7.03 (bs, 1H), 4.59 (d, *J* = 6.4 Hz, 2H). This product was reacted with 2-chlorobenzoyl chloride according to the procedure provided for 2,4-dibromo-6-((2 nitrobenzamido)methyl)phenyl 2-chlorobenzoate, affording 4.2 mg of the desired product (6.5% yield). ^{1}H NMR (400 MHz, $CDCl_3$) δ 8.97 (s, 1H), 8.71 (s, 1H), 8.21 (dd, 1H), 8.07 (d, *J* = 8.1 Hz, 1H), 7.77 (d, *J* = 2.3 Hz, 1H), 7.62 (d, *J* = 2.3 Hz, 1H), 7.58 – 7.50 (m, 2H), 7.47 – 7.39 (m, 1H), 7.39 – 7.33 (m, 1H), 6.80 (t, 1H), 4.63 (s, 2H). ^{13}C NMR (101 MHz, $CDCl_3$) δ 165.40, 163.37, 152.55, 148.24, 146.10, 135.58, 135.21, 135.00, 134.32, 132.79, 132.64, 131.74, 127.52, 127.17, 123.63, 120.52, 118.19, 39.50. ESI-MS calculated for $C_{20}H_{14}Br_2ClN_2O_5$, 522.91 [M+H], observed 522.97. HPLC purity 89.5%.

5.1.36. 2,4-Dibromo-6-(picolinamidomethyl)phenyl 4-(2,5-dioxo-2,5-dihydro-1H-pyrrol-1-yl)butanoate, ***42****.*

Prepared according to the procedure provided for 2,4-dibromo-6-((2 nitrobenzamido)methyl)phenyl 2-chlorobenzoate from *N*-(3,5-dibromo-2-hydroxybenzyl)picolinamide, affording 35.7 mg of the desired product (25.1% yield). ^{1}H NMR (400 MHz, $CDCl_3$) δ 8.53 (dd, *J* = 4.8, 1.3 Hz, 1H), 8.41 (s, 1H), 8.19 (dd, *J* = 7.8, 1.2 Hz, 1H), 7.86 (td, *J* = 7.7, 1.7 Hz, 1H), 7.66 (d, *J* = 2.3 Hz, 1H), 7.53 (d, *J* = 2.3 Hz, 1H), 7.47 – 7.39 (m, 1H), 6.72 (s, 2H), 4.59 (d, *J* = 6.4 Hz, 2H), 3.68 (t, *J* = 6.7 Hz, 2H), 2.70 (t, *J* = 7.3 Hz, 2H), 2.10 – 1.98 (m, 2H). ^{13}C NMR (101 MHz, $CDCl_3$) δ 170.94, 170.02, 164.39, 149.49, 148.32, 146.02, 137.56, 134.94, 134.82, 134.31, 132.05, 126.56, 122.53, 119.96, 118.15, 38.75, 36.98, 31.20, 23.79. ESI-MS calculated for $C_{21}H_{18}Br_2N_3O_5$, 549.96 [M+H], observed 549.92. HPLC purity 89.7%.

5.1.37. (S)-2-(3,5-Dibromo-2-hydroxyphenyl)-N-(2-oxotetrahydrofuran-3-yl)acetamide.

To a solution of 2-(3,5-dibromo-2-hydroxyphenyl)acetic acid (0.750g, 2.42mmol) and L-Homoserine lactone hydrobromide (0.881g, 4.84mmol) in DMF (12.1mL) was added HATU (1.103g, 2.90mmol) followed by i-Pr_2NEt (1.3mL, 7.26mmol). The resulting mixture was allowed to stir at room temperature overnight, was diluted with EtOAc, washed with water, 1M HCl and brine, dried over Na_2SO_4 and concentrated to dryness. The residue was purified by flash column chromatography using a gradient from hexanes to EtOAc to provide the desired product (0.430g, 45%). ^{1}H-NMR (400 MHz, Chloroform-d) δ 8.68 (s, 1H), 7.55 (d, J = 2.3 Hz, 1H), 7.21 (d, J = 2.3 Hz, 1H), 6.92 (d, J = 6.1 Hz, 1H), 4.61-4.52 (m, 1H), 4.48 (t, J = 9.1 Hz, 1H), 4.36-4.25 (m, 1H), 3.62 (ABq, $\Delta\nu_{AB}$ = 11.3 Hz, J_{AB} = 12.3 Hz, 2H), 2.85-2.75 (m, 1H), 2.25-2.11 m, 1H).

5.1.38. 2,4-Dibromo-6-(2-oxo-2-((2-oxotetrahydrofuran-3-yl)amino)ethyl)phenyl 4-(2,5-dioxo-2,5-dihydro-1H-pyrrol-1-yl)butanoate, ***43****.*

Prepared according to the procedure provided for 2,4-dibromo-6-(2-((2-nitrophenyl)amino)-2-oxoethyl)phenyl 2-chlorobenzoate from (*S*)-2-(3,5-dibromo-2-hydroxyphenyl)-*N*-(2-oxotetrahydrofuran-3-yl)acetamide, affording 12.5 mg of the desired product (61% yield). ^{1}H NMR (400 MHz, Chloroform-d) δ 7.67 (d, J = 2.3 Hz, 1H), 7.58 (d, J = 2.3 Hz, 1H), 7.14 (s, 1H), 6.77 (s, 2H), 4.59 – 4.48 (m, 1H), 4.44 (t, 1H), 4.32 – 4.21 (m, 1H), 3.77 – 3.64 (m, 2H), 2.89 – 2.79 (m, 1H), 2.84 – 2.67 (m, 2H), 2.20 – 2.01 (m, 2H). ^{13}C NMR (101 MHz, Chloroform-d) δ 175.30, 171.77, 170.42, 169.82, 134.90, 134.56, 134.06, 131.72, 120.02, 66.36, 49.73, 37.50, 36.68, 31.16, 30.62, 30.51, 23.69. ESI-MS calculated for $C_{20}H_{19}Br_2N_2O_7$, 556.96 [M+H], observed 556.81. HPLC purity 92.5%.

5.1.39. 2,4-Dibromo-6-(2-oxo-2-((2-oxotetrahydrofuran-3-yl)amino)ethyl)phenyl 3-(2,5-dioxo-2,5-dihydro-1H-pyrrol-1-yl)propanoate, ***44****.*

Prepared according to the procedure provided for 2,4-dibromo-6-(2-((2-nitrophenyl)amino)-2-oxoethyl)phenyl 2-chlorobenzoate from (*S*)-2-(3,5-dibromo-2-hydroxyphenyl)-*N*-(2-oxotetrahydrofuran-3-yl)acetamide, affording 1.8 mg of the desired product (17% yield). ^{1}H NMR (400 MHz, Chloroform-d) δ 7.68 (d, J = 2.2 Hz, 1H), 7.53 (d, J = 2.2 Hz, 1H), 6.75 (s, 1H), 4.60 – 4.48 (m, 1H), 4.46 (t, J = 9.1 Hz, 1H), 4.33 – 4.21 (m, 1H), 4.15 – 3.91 (m, 2H), 3.62 – 3.47 (m, 2H), 3.12 – 2.97 (m, 2H), 2.83 – 2.71 (m, 0H), 2.75 (s, 1H), 2.25 – 2.09 (m, 1H), 1.38 – 1.23 (m, 2H), 0.89 (d, J = 12.6 Hz, 1H). ^{13}C NMR (101 MHz, Chloroform-d) δ 175.23, 170.84, 169.52, 168.71, 146.18, 135.12, 134.60, 133.71, 131.50, 120.34, 118.19, 66.27, 49.62, 37.96, 33.58, 32.69, 31.85, 30.08, 29.87. ESI-MS calculated for $C_{19}H_{17}Br_2N_2O_7$, 542.94 [M+H], observed 542.92. HPLC purity 91.8%.

5.2. LasR Bioassay

The LasR reporter strain bioassay was performed as described previously with modifications.[23] Briefly, the assays were performed in *E. coli* strain BL21 DE3 Gold (Agilent) carrying a plasmid containing *lasR* (maintained with 100 μg/mL ampicillin) and a plasmid containing the *rsaL* promoter-driving expression of *gfp* (maintained with 50 μg/mL of kanamycin.) The reporter strain described above was kindly supplied by Bonnie L. Bassler (Princeton University). This *E. coli* strain was grown overnight at 37°C in Luria broth (LB) (Fisher) with the appropriate antibiotics. The overnight culture was subcultured 1:40 for bioassay analysis. The native LasR agonist, *N*-3-oxo-dodecanoyl-L-homoseriene lactone was used as a positive control for all agonist assays (EC_{50}=72.9±24.6nM) and was employed at a constant concentration of 50nM for all antagonist assays. For agonists assays, maximal % activation is reported with respect to *N*-3-oxo-dodecanoyl-L-homoseriene lactone set as 100% activation. For antagonism assays, the previously described antagonist, (*S*)-2-(4-bromophenyl)-*N*-(2-oxotetrahydrofuran-3-yl) acetamide was used as the positive control for antagonism with an IC_{50} of 26.31±15.7μM.[8] Maximal % inhibition is reported with respect to (*S*)-2-(4-bromophenyl)-*N*-(2-oxotetrahydrofuran-3-yl) acetamide set as 100% inhibition. Compounds were added to the diluted overnight reporter strain in 96-well black microplates with clear bottoms (Corning) at the starting concentrations described and titrated by serial dilution. Plates were incubated with shaking at 37°C for 4-6h and were evaluated for fluorescence (ex485/em538) and absorbance (A_{600}) using a Molecular Devices SpectraMax M5 microplate reader, or a FlexStation II 384 Molecular Devices for fluorescence and a MultiSkan Spectrum for absorbance measurements. Dose-response curves were fit to the data using standard nonlinear regression data fitting settings in GraphPad Prism 6, no corrections for compound purity were made. All data points are reported as mean with error describing the standard deviation.

5.3. Computational Modeling

5.3.1. Ligand Preparation.

The triaryl series of ligands were prepared using first Maestro Elements then Maestro 10.3. The 2D structures were draw using the 2D sketcher function in Maestro Elements. The templates for

the ligands were obtained from the Perez Lab. The 2D sketches were then converted to 3D structures. Epik (an empirical pka prediction program) was utilized to determine the charge of the molecule at pH 7.[24] Finally, the 3D structures were uploaded into the Maestro 10.3 and restrained minimization was run. This function is used to relax and optimize the ligand structure.

5.3.2. Protein structure Preparation.

The LasR crystal structure (PDB 3IX3) was prepared using the protein preparation wizard function in Maestro. The charge state of preprocessed protein was optimized at pH=7. Finally restrained minimization was performed to relax the protein structure using OPLS3 force field.[25]

5.3.3. Ligand Docking.

The individual ligands were docking using glide docking with extra precision (XP) and default parameters.[26,27] The receptor grid required for docking process was generated using Van der Waals scaling factor of 1 and partial charge cutoff 0.25. Docking was performed using a ligand-centered grid using OPLS3 force field. The Glide XP Dock function performs a comprehensive systematic search for the best receptor conformations and orientations to fit the ligand. To validate the docking method, the crystal ligand of of 3-OXO-C12-HSL was docked back to the pocket. The small heavy atom RMSD of 0.6Å between the docked pose and the crystal pose indicates the validity of the docking method (see online supporting information, Figure S1).

5.3.4. Binding energy Calculations and decompositions methods.

Molecular Mechanism-General Born Surface Area (MM-GBSA) binding energies were calculated on the complexes from the docking. OPLS3 force field[25], VSGB 2.0 solvation model[28] and the default Prime procedure was used for the MM-GBSA calculation. The default procedure consists of three steps: Receptor alone (minimization), Ligand alone (minimization), Receptor-ligand complex (minimization). The total binding energy equation is: $\Delta G_{(bind)} = E_{complex(minimized)} - (E_{ligand(minimized)} + E_{receptor(minimized)}$. The docked complex with the MM-GBSA binding energy is listed in Figure S2 of the online supporting information. The residue breakdown of the $\Delta G_{(bind)}$ were then used in combination with 2D interaction diagrams to identify and compare key residues within the binding pocket. Note that since the binding entropy is not included in our analysis, the binding energies by MMGBSA may over-estimate the binding free energy (i.e. the binding affinity). But when the entropic term of different ligands are comparable, the relative MMGBSA binding energies can be used to estimate the relative binding free energy for ranking ligands.[29] The correlation coefficient between the experimental binding free energy (calculated from the EC_{50}) and the MMGBSA binding energies is 0.5572, which is reasonable (see online supporting information, Figure S3).

Acknowledgements

The authors would like to acknowledge Izaz Kazmi for assistance in the synthesis of analogs **33** and **35**; Joseph G. Noto and Kevin T. O'Brien for assistance in the synthesis of analogs **20**, **24** and **29**. Financial support was provided by Rowan University CSM and SEED grants and by a Rowan University New Faculty Research Startup Grant.

Supplementary data

Supplemental figures, ^{1}H-NMR and ^{13}C-NMR spectra for all new compounds and dose-response curves for biological activity data associated with this article can be found in the online version.

References and notes

1. Lesic, B.; Lépine, F.; Déziel, E.; Zhang, J.; Zhang, Q.; Padfield, K.; Castonguay, M.-H.; Milot, S.; Stachel, S.; Tzika, A. A.; Tompkins, R. G.; Rahme, L. G. *PLoS Pathog.* **2007**, *3*, 1229–1239.
2. Rasmussen, T. B.; Givskov, M. *Int. J. Med. Microbiol.* **2006**, *296*, 149–161.
3. Lyon, G. J.; Muir, T. W. *Chemistry & Biology* **2003**, *10*, 1007–1021.
4. Manefield, M.; de Nys, R.; Kumar, N.; Read, R.; Givskov, M.; Steinberg, P.; Kjelleberg, S. *Microbiology (Reading, Engl.)* **1999**, *145 (Pt 2)*, 283–291.
5. Müh, U.; Hare, B. J.; Duerkop, B. A.; Schuster, M.; Hanzelka, B. L.; Heim, R.; Olson, E. R.; Greenberg, E. P. *Proc. Natl. Acad. Sci. U.S.A.* **2006**, *103*, 16948–16952.
6. Müh, U.; Schuster, M.; Heim, R.; Singh, A.; Olson, E. R.; Greenberg, E. P. *Antimicrobial Agents and Chemotherapy* **2006**, *50*, 3674–3679.
7. Geske, G. D.; O'Neill, J. C.; Miller, D. M.; Wezeman, R. J.; Mattmann, M. E.; Lin, Q.; Blackwell, H. E. *ChemBioChem* **2008**, *9*, 389–400.
8. Geske, G. D.; O'Neill, J. C.; Miller, D. M.; Mattmann, M. E.; Blackwell, H. E. *J. Am. Chem. Soc.* **2007**, *129*, 13613–13625.
9. Mattmann, M. E.; Blackwell, H. E. *J. Org. Chem.* **2010**, *75*, 6737–6746.
10. Moore, J. D.; Rossi, F. M.; Welsh, M. A.; Nyffeler, K. E.; Blackwell, H. E. *J. Am. Chem. Soc.* **2015**, *137*, 14626–14639.
11. Lambert, P. A. *Journal of the Royal Society of Medicine* **2002**, *95*, 22.
12. Kollef, M. H.; Golan, Y.; Micek, S. T.; Shorr, A. F.; Restrepo, M. I. *CLIN INFECT DIS* **2011**, *53*, S33–S55.
13. Defoirdt, T.; Boon, N.; Bossier, P. *PLoS Pathog.* **2010**, *6*, e1000989.
14. Khmel, I. A.; Metlitskaya, A. Z. *Mol Biol* **2006**, *40*, 169–182.
15. Clatworthy, A. E.; Pierson, E.; Hung, D. T. *Nat Chem Biol* **2007**, *3*, 541–548.
16. Rasko, D. A.; Sperandio, V. *Nature Reviews Drug Discovery* **2010**, *9*, 117–128.
17. Hentzer, M.; Wu, H.; Andersen, J. B.; Riedel, K.; Rasmussen, T. B.; Bagge, N.; Kumar, N.; Schembri, M. A.; Song, Z.; Kristoffersen, P.; Manefield, M.; Costerton, J. W.; Molin, S.; Eberl, L.; Steinberg, P.; Kjelleberg, S.; Høiby, N.; Givskov, M. *EMBO J.* **2003**, *22*, 3803–3815.
18. O'Reilly, M. C.; Blackwell, H. E. *ACS Infect Dis* **2016**, *2*, 32–38.
19. Zakhari, J. S.; Kinoyama, I.; Struss, A. K.; Pullanikat, P.; Lowery, C. A.; Lardy, M.; Janda, K. D. *J. Am. Chem. Soc.* **2011**, *133*, 3840–3842.
20. Zou, Y.; Nair, S. K. *Chemistry & Biology* **2009**, *16*, 961–970.
21. Meanwell, N. A. *J. Med. Chem.* **2011**, *54*, 2529–2591.
22. O'Brien, K. T.; Noto, J. G.; Nichols-O'Neill, L.; Perez, L. J. *ACS Med Chem Lett* **2015**, *6*, 162–167.
23. O'Loughlin, C. T.; Miller, L. C.; Siryaporn, A.; Drescher, K.; Semmelhack, M. F.; Bassler, B. L. *Proc. Natl. Acad. Sci. U.S.A.* **2013**, *110*, 17981–17986.
24. Sastry, G. M.; Adzhigirey, M.; Day, T.; Annabhimoju, R.; Sherman, W. *J. Comput. Aided Mol. Des.* **2013**, *27*, 221–234.
25. Harder, E.; Damm, W.; Maple, J.; Wu, C.; Reboul, M.; Xiang, J. Y.; Wang, L.; Lupyan, D.; Dahlgren, M. K.;

Knight, J. L.; Kaus, J. W.; Cerutti, D. S.; Krilov, G.; Jorgensen, W. L.; Abel, R.; Friesner, R. A. *J Chem Theory Comput* **2016**, *12*, 281–296.
26. Friesner, R. A.; Murphy, R. B.; Repasky, M. P.; Frye, L. L.; Greenwood, J. R.; Halgren, T. A.; Sanschagrin, P. C.; Mainz, D. T. *J. Med. Chem.* **2006**, *49*, 6177–6196.
27. Friesner, R. A.; Banks, J. L.; Murphy, R. B.; Halgren, T. A.; Klicic, J. J.; Mainz, D. T.; Repasky, M. P.; Knoll, E. H.; Shelley, M.; Perry, J. K.; Shaw, D. E.; Francis, P.; Shenkin, P. S. *J. Med. Chem.* **2004**, *47*, 1739–1749.
28. Li, J.; Abel, R.; Zhu, K.; Cao, Y.; Zhao, S.; Friesner, R. A. *Proteins* **2011**, *79*, 2794–2812.
29. Kongsted, J.; Söderhjelm, P.; Ryde, U. *J. Comput. Aided Mol. Des.* **2009**, *23*, 395–409.